Published in final edited form as:
Nat Immunol. 2020 August 01; 21(8): 927–937. doi:10.1038/s41590-020-0714-5.

Dynamics in protein translation sustaining T cell preparedness

Tobias Wolf[#1,2], **Wenjie Jin**[#1], **Giada Zoppi**[1], **Ian A. Vogel**[1], **Murodzhon Akhmedov**[1], **Christopher K.E. Bleck**[3], **Tim Beltraminelli**[1], **Jan C. Rieckmann**[4], **Neftali J. Ramirez**[5,6], **Marco Benevento**[1], **Samuele Notarbartolo**[1], **Dirk Bumann**[3], **Felix Meissner**[4,7], **Bodo Grimbacher**[5,8,9,10], **Matthias Mann**[11], **Antonio Lanzavecchia**[1], **Federica Sallusto**[1,2], **Ivo Kwee**[1], **Roger Geiger**[1,§]

[1]Institute for Research in Biomedicine, Università della Svizzera italiana, Switzerland [2]Institute of Microbiology, ETH Zürich, Switzerland [3]Biozentrum, University of Basel, Switzerland [4]Max Planck Institute of Biochemistry, Experimental Systems Immunology, Germany [5]Institute for Immunodeficiency, Center for Chronic Immunodeficiency, Medical Center, Faculty of Medicine, Albert-Ludwigs-University of Freiburg, Freiburg, Germany [6]Integrated Research Training Group (IRTG) Medical Epigenetics, Collaborative Research Centre 992, Freiburg, Germany [7]Institute of Innate Immunity, Department of Systems Immunology and Proteomics, Medical Faculty, University of Bonn [8]DZIF – German Center for Infection Research, Satellite Center Freiburg, Germany [9]CIBSS – Centre for Integrative Biological Signalling Studies, Albert-Ludwigs University, Freiburg, Germany [10]RESIST – Cluster of Excellence 2155 to Hanover Medical School, Satellite Center Freiburg, Germany [11]Max Planck Institute of Biochemistry, Department of Proteomics and Signal Transduction, Germany

[#] These authors contributed equally to this work.

Abstract

In response to pathogenic threats, naïve T cells rapidly transition from a quiescent to activated state, yet the underlying mechanisms are incompletely understood. Using a pulsed SILAC approach, we investigated the dynamics of mRNA translation kinetics and protein turnover in human naïve and activated T cells. Our datasets uncovered that transcription factors maintaining T cell quiescence had constitutively high turnover, which facilitated their depletion upon activation. Furthermore, naïve T cells maintained a surprisingly large number of idling ribosomes as well as 242 repressed mRNA species and a reservoir of glycolytic enzymes. These components were

[§]Correspondence to roger.geiger@irb.usi.ch.

Author Contributions

R.G. conceived the study, designed experiments, analyzed data and wrote the manuscript. T.W., W.J., G.Z., I.A.V., J.C.R. designed and performed experiments with human T cells. M.A. and I.K. wrote the R shiny code for the online platform. M.B. helped with mass spectrometry. C.K.E.B. and T.B. performed theelectron microscopy and analysis. N.J.R. did ATAC-Seq and S.N. ChIP-Seq analysis. D.B., F.M., B.G., M.M., A.L., F.S., I.K. and R.G. supervised the work.

Competing Interests

The authors declare no competing interests.

Reporting Summary

Further information on research design is available in the Nature Research Reporting Summary linked to this article.

Europe PMC Funders Author Manuscripts

rapidly engaged following stimulation, promoting an immediate translational and glycolytic switch to ramp up the T cell activation program. Our data elucidate new insights into how T cells maintain a prepared state to mount a rapid immune response, and provide a resource of protein turnover, absolute translation kinetics and protein synthesis rates in T cells (www.immunomics.ch).

Introduction

Resting T cells patrol the body in a quiescent yet poised state, prepared to mount a robust immune response to pathogenic threats such as infectious diseases and cancers. Naïve T cells may remain inactive for many years in a spore-like state[1, 2]. While surveying for cognate antigen, quiescent T cells maintain a cellular program with minimal energy expenditure[3, 4]. However, following activation T cells need to rapidly undergo a substantial reprogramming to mount an effective response[5]. Thus, T cells face a tradeoff between minimizing their metabolic activity while sustaining a maximally prepared state for rapid execution of the activation program.

In response to an antigenic stimulus, T cells exit quiescence and rewire their transcriptional and metabolic programs. Activated T cells ramp up their translational activity[6], increase nutrient uptake[7] and rapidly engage glycolysis to provide energy and building blocks that support cell growth, proliferation and the acquisition of effector functions[7, 8, 9]. The extensive reprogramming of activated T cells is increasingly well understood owing to epigenomic, metabolomic, transcriptomic and proteomic analyses[10, 11, 12, 13, 14]. However, translational dynamics and protein turnover in T cells have not been investigated.

In this study, we examined the dynamics of protein synthesis and turnover in human T cells using pulsed SILAC-based high-resolution mass spectrometry[15, 16, 17, 18]. We identified several key proteins that were rapidly renewed in naïve T cells, which maintained quiescence.Intrinsically high turnover in naïve T cells facilitated their rapid depletion following stimulation to enable exit of quiescence. Our data also revealed that naïve T cells contained large numbers of idling ribosomes that were rapidly engaged following stimulation to ramp up the activation program. In addition, naïve T cells also maintained a reservoir of repressed mRNAs, which were translated following activation. Finally, although naïve T cells exhibited very low glycolytic activity, 11% of their cytosolic proteins were glycolytic enzymes, which were immediately engaged following T cell activation to increase aerobic glycolysis. Together these findings define molecular underpinnings of T cell preparedness, licensing T cells with the ability to rapidly undergo activation.

Results

Naïve T cells rapidly renew a small set of proteins

To measure protein synthesis and turnover rates we employed a pulsed SILAC approach where T cells are cultured for increasing times in a medium containing stable isotope labeled amino acids Arg10 and Lys8 (hereafter referred to as heavy amino acids). Under these conditions, newly translated proteins incorporate heavy amino acids and can be

Europe PMC Funders Author Manuscripts

distinguished from pre-existing proteins by a mass shift (Fig. 1a).Given that non-activated T cells remain quiescent and do not grow nor divide, the total proteome mass remains constant over time (Extended Data Fig. 1a). As such, newly synthesized proteins do not contribute to cell growth but replenish their degraded counterparts. Hence, protein synthesis in naive T cells is a proxy for protein renewal.

First, naïve $CD45RA^+$ $CCR7^+$ $CD4^+$ T cells were isolated to high purity (>98%) from peripheral blood mononuclear cells (PBMCs) of four healthy donors and cultured without a stimulus in a medium containing heavy amino acids. The cell viability was higher than 90% after 48 h of culturing (Extended Data Fig. 1b). Samples were collected after 0, 6, 12, 24, and 48 h, and analyzed by liquid chromatography-coupled high-resolution mass spectrometry (LC-MS). We quantified 7,029 proteins and calculated protein renewal rates based on the MS signal intensities of total and newly synthetized proteins.

After a 6 h pulse, 205 protein species were detected that incorporated heavy amino acids. Strikingly, at this early time point several components of MHC-I (HLA-A, HLA-B, HLA-C, HLA-G, HLA-E and β_2M) as well as the transcription factor ETS-1 were already renewed by more than 80% as judged by the percentage of proteins that incorporated heavy amino acids (Fig. 1b). After a 24 h pulse, the number of renewed protein species that were reliably identified in three out of four donors increased to 1,313, which is 19% of all protein species in naïve T cells (Fig. 1c, Supplementary Table 1). Among the 23 protein species with the fastest renewal rates (>90% after 24h) were SORL1, SQSTM1, and transcriptional regulators, including ETS1, TCF-1 AES, FOXO1, FOXP1, LEF1, ELF1, PBXIP1, and LBH.

By fitting the renewal rates of different time points to a Weibull distribution, we estimated half-lives of 1,822 out of 7,029 identified proteins. The fastest renewed proteins had a half-life of less than one hour, i.e. 45 min for β_2M and 53 min for ETS1 (Fig. 1d, www.immunomics.ch). Examples with an intermediate turnover rate were the T cell receptor subunits CD3δ, CD3γ, CD3ε and CD247 ($t_{1/2}$ = 11 - 14 h), which displayed a similar renewal rate (Fig. 1c,d). Examples with slow turnover were the ribosomal protein RPL8 ($t_{1/2}$ = 260 h) and the glycolytic enzyme GAPDH ($t_{1/2}$ = 210 h). Slowest turnover rates were observed for several histones ($t_{1/2}$ > 1,000 h), suggesting that nucleosomes were stable in naïve T cells. Taken together, most protein species in naïve T cells were stable, or only slowly renewed, while a small set of proteins was renewed within only a few hours.

Constitutive protein degradation in naïve T cells

Protein turnover is the net result of protein synthesis and degradation.To further validate that proteins for which we found high turnover rates are also rapidly degraded, we quantified protein degradation rates using cycloheximide (CHX), a reversible inhibitor of the ribosome. Resting naïve T cells were treated for 24 h with CHX and then analyzed by LC-MS. A comparison of their proteome to non-treated cells identified those proteins that were constitutively degraded as they largely disappeared in the absence of protein synthesis. Notably, the vast majority of proteins that decreased in abundance were of high turnover, as determined by pulsed SILAC (Fig.2a, color-code of the dots shows the renewal rate). For example, ETS1 and SORL1, which were among the fastest renewed proteins in naive T

cells, were both strongly reduced following inhibition of translation (Fig.2a and 1c), validating our approach for quantifying protein turnover.

To identify which proteins were constitutively degraded by the proteasome, we simultaneously treated naïve T cells for 24 h with CHX and bortezomib (PS341), a specific inhibitor of the proteasome (Extended Data Fig 1c). We then analyzed proteomes and estimated absolute protein copy numbers using a previously described method[19]. While the abundancex of SQSTM1, a cargo receptor for selective autophagy[20], as well as the plasma membrane proteins SORL1, HLA-A, HLA-B, β_2M and CD62L were reduced in the presence of CHX, simultaneous addition of CHX and bortezomib did not stabilize these proteins, suggesting that they were degraded through a proteasome-independent pathway (Fig. 2b). In contrast, the degradation of the transcription factors and regulatory proteins ETS1, FOXP1, TCF-1, LEF1, ELF1, LBH, AES, PBXIP1, FAM65B, STK17B was stabilized by bortezomib, indicating that they were constitutively degraded by the proteasome (Fig. 2c). This analysis further revealed that TXNIP, which suppresses glucose uptake[21] and KLF2, a transcription factor that controls the expression of chemokine receptors and adhesion molecules that regulate T cell trafficking[22], were constitutively degraded by the proteasome in naive T cells (Fig. 2c). Due to their low abundance (200 - 2,000 copies), TXNIP and KLF2 were not reliably identified in the pulsed SILAC experiments. Taken together, membrane proteins with high turnover were degraded through a proteasome-independent pathway, likely in endosomes / autophagosomes, whereas the rapidly renewed transcription factors and regulatory proteins were degraded by the proteasome.

As shown in the previous experiments, inhibition of protein synthesis in naïve T cells with CHX for 24 h led to a decrease in the abundance of β_2M and HLA-ABC proteins by about 50%, from ~500,000 to ~225,000 copies and from ~380,000 to ~190,000 copies, respectively (Fig. 2b). We next treated naïve T cells with CHX and followed surface MHC-I protein abundance by flow cytometry. Consistent with the proteomics data, surface MHC-I decreased about 50% within 24 h (Fig. 2d). Notably, following wash-out of CHX, MHC-I surface abundance was completely restored in less than 6 h, confirming that naïve T cells rapidly synthesize large amounts of MHC-I components.

To rule out possible artifacts caused by CHX, we used a CRISPR/Cas9 approach to disrupt the *B2M* gene in resting naïve T cells. Freshly isolated naïve $CD4^+$ T cells were electroporated with ribonucleoprotein (RNP) complexes consisting of ATTO550-labeled trans-activating CRISPR (tracr) RNA, Cas9 protein and guide RNAs targeting two independent sites of *B2M*.The abundance of MHC-I at the cell surface was reduced already after 24 h in greater than 90% of naïve T cells that had taken up the RNP ($ATTO550^+$). By 72 h,MHC-I surface abundance further decreased as judged by a reduction in mean fluorescence intensity (MFI; Fig. 2e). Together, these results confirm that MHC-I is continuously degraded and replenished in naïve T cells.

Transcription factors display a high turnover

Cell identity and function are largely determined by transcription factors. The half-lives of transcription factors in naïve T cells ranged from 53 min to 126 h (Fig. 3a), raising the

question whether transcription factors with high turnover play a defining role in the cell state. The fastest renewed transcription factor in naïve T cells was ETS1, which plays an essential role in maintaining T cell homeostasis[23, 24]. To corroborate ETS1 activity in naïve human T cells, we generated a genome-wide map of chromatin accessibility in purified resting naïve $CD4^+$ T cells from three donors using the assay for transposase-accessible chromatin (ATAC-seq)[25]. We identified a total of 34,370 distinct chromatin accessibility peaks of which 13,592 were located in promoter regions (Extended Data Fig. 2a, Supplementary Table 2). Notably, the transcription factor binding motifs that were enriched the most in these regions were recognized by ETS1 ($P = 10^{-64}$). To confirm broad DNA binding of ETS1, we performed ChIP-seq analysis for genome-wide binding of ETS1 in purified T cells. ETS1 was bound at 11,222 sites in the genome that were associated with over 9,688 genes (Supplementary Table 3). 50% of the ETS1 binding sites were in promoter regions suggesting direct ETS1 mediated transcriptional regulation (Extended Data Fig. 2b). Collectively, ETS1, which has the highest turnover of any transcription factor in naïve T cells,has broad binding activity and thus plays a defining role in the cell state.

High protein turnover facilitates T cell reprogramming

Perpetual degradation and re-synthesis of proteins is an energy consuming process. However, high turnover of specific proteins allows for rapid fine-tuning of their abundance, facilitating an immediate adaptation of the cellular program in response to various stimuli. In general, a decrease in mRNA transcript abundance encoding proteins with high turnover results in their immediate depletion, whereas proteins with low turnover are not as promptly responsive to decreased transcription. We therefore explored whether T cells rely on high protein turnover in steady-state conditions for rapid reprogramming in response to different stimuli.

We quantified absolute and relative protein abundances immediately following activation of naïve T cells with plate-bound anti-CD3 and anti-CD28 antibodies. This resulted in a comprehensive and dynamic dataset on proteomes of naïve and activated T cells (7,772 quantified proteins).Interestingly, we observed that the rapidly renewed proteins FAM65B, KLF2, TCF-1, TXNIP, SORL1, PBXIP1 and CD247 were down regulated early after activation (Fig. 3b). For example, loss of KLF2 is necessary to acquire T cell effector function while down-regulation of FAM65B promotes exit of quiescence[3, 26]. For comparison, examples with an opposite pattern were β_2M and NF-$_{\kappa B1}$, the slowest renewed transcription factor in naïve T cells (Fig. 3a,b). Taken together, several proteins responsible for maintaining T cell quiescence had constitutively high turnover in naïve T cells and were rapidly down-regulated upon activation.

To further explore whether some rapidly renewed proteins are down-regulated in activated T cells *in vivo*, we analyzed tumor-infiltrating T cells (TILs), which respond to antigenic stimulation and other signals in the tumor microenvironment (TME)[27] (Extended Data Fig. 2c). We compared transcriptomes of TILs and circulating T cells from patients with hepatocellular carcinoma (HCC)[28]. Interestingly, the vast majority of mRNAs that were down-regulated in TILs encoded proteins that are rapidly renewed in resting T cells, including KLF2, LEF1, TCF-1, FOXP1, AES, TXNIP, FAM65B, SORL1 and CD62L (Fig.

Europe PMC Funders Author Manuscripts

3c). Thus, several key proteins depleted in the TME were maintained at high turnover in resting T cells, suggesting protein turnover is an important factor in facilitating T cell responsiveness.

Pre-existing glycolytic enzymes in naïve T cells

As metabolic reprogramming is a requirement for the exit of quiescence, we compared turnover of glycolytic enzymes in naïve and activated T cells implementing the pulsed SILAC approach. Estimating protein turnover in activated T cells with the pulsed SILAC method is only possible for proteins whose abundances remain constant following activation. Therefore, we first sought to identify glycolytic enzymes in T cells whose abundance does not change within 12 h of activation. Surprisingly, although glycolysis markedly increased early after activation (Extended Data Fig. 3a), the only enzyme that was strongly upregulated was hexokinase-2 (HK2), while all other glycolytic proteins did not change in abundance during the first 12 h after activation (Fig. 4a). Although naïve T cells have low glycolytic activity, they contained millions of copies of glycolytic enzymes (11% of all cytosolic proteins, Extended Data Fig. 3b). For each reaction step in the glycolytic pathway, naïve T cells already had highly abundant enzymes (Fig.4b, in blue). Thus, upon activation naïve T cells increase the expression of HK2, engage a large pool of pre-existing enzymes and concomitantly increase their glycolytic activity.

Having established that nearly all glycolytic enzymes remain constant in abundance early after activation, we determined protein turnover rates in T cells that were activated for 6 h and 12 h in the presence of heavy amino acids. Strikingly, the turnover of all measured glycolytic enzymes substantially increased 12 h after activation (Extended Data Fig. 3c). For example, naïve T cells contained ~1.3 million copies of lactate dehydrogenase A (LDHA), of which 6.5% were renewed within 12 h in resting naïve T cells (Fig.4c). In contrast, 12 h after activation the fraction of renewed LDHA increased to 65% while the total amount of LDHA remained steady (~1.4 million copies), (Fig. 4c, examples are also shown for GAPDH, ALDOA, PGK1). In conclusion, naïve T cells contain large pools of glycolytic enzymes whose activity and turnover markedly increase following activation.

Pre-existing, idle ribosomes in naïve T cells

Naïve T cells only have a thin layer of cytoplasm with a volume of 82.5 ± 9 fl as determined by serial block-face scanning electron microscopy and subsequent 3D reconstruction of images. Following activation T cells expand their cytoplasm to 670 ± 74 fl (Fig. 5a-d and Extended Data Fig. 4), which requires a substantial increase in protein synthesis. We implemented an algorithm to compare the ribosomal output in naïve and activated T cells by further analyzing the pulsed SILAC datasets. Absolute protein synthesis rates (copy numbers min^{-1}) were calculated as total protein copy numbers multiplied by the fraction of heavily labeled proteins over time. We found that naive T cells synthetized in total ~60,000 proteins min^{-1}, a result that was consistently found independent of the duration of the pulse with heavy amino acids. After 6 h of activation, protein synthesis rates increased to ~300,000 proteins min^{-1} and after 24 h to ~800,000 proteins min^{-1} (Fig. 5e). Thus, the ribosomal output increased more than 13-fold following activation.

In naïve T cells, the proteins with the highest synthesis rates were β_2M with a median of ~4,300 copies min^{-1} followed by β-actin, clusterin, ubiquitin and HLA-A (~4,000, ~2,900, ~2,300 and ~2,000 copies min^{-1}, respectively) (Fig. 5f). In 24 h-activated T cells, β-actin had the highest median synthetic rate of 54,000 copies min^{-1}, which was nearly equivalent to the entire synthesome of naïve T cells (Fig. 5g).

We next estimated the number of ribosomes using two orthogonal approaches that were based on copy number estimations of ribosomal proteins and on quantifications of ribosomal RNA (Fig. 5h and Extended Data Figs. 5a-c). This revealed that naïve T cells contained enough ribosomal proteins and rRNAs to assemble ~400,000 ribosomes. Based on estimated numbers of ribosomes and absolute protein synthesis rates, we calculated an average output per ribosome of ~0.8 amino acids sec^{-1} in naïve T cells (Fig. 5i).Strikingly, 6 h after T cell activation the average output per ribosome increased 5-fold to ~4.0 amino acids sec^{-1}. These data demonstrate that naïve T cells contain large numbers of idling ribosomes that are rapidly engaged following activation to promote a translational switch.

Repressed mRNAs are rapidly translated after activation

To investigate whether the rapid increase in the ribosomal output following T cell activation was regulated transcriptionally, we analyzed transcriptomes of naïve resting and activated T cells by RNA-Seq and established an algorithm to estimate absolute mRNA copy numbers.In contrast to the proteome consisting of ~410 million proteins, naïve T cells contained only ~77,000 mRNA molecules (Supplementary Table 4, individual mRNA species in naïve T cells ranged from <1 to 3,700 mRNA copies). On average, this corresponds to a mRNA to protein ratio of 1 to 5,400 (Extended Data Fig. 5d). 6 h following activation, the total number of mRNAs only increased 1.4-fold to 105,000 transcripts, indicating that the 5-fold increase in the ribosomal output was predominately regulated at the post-transcriptional level (Extended Data Figs. 5e-f).

A comparison between mRNA copy numbers and protein synthetic rates revealed a Spearman's rank correlation of 0.41 in naïve T cells. 6 h following activation, the correlation between transcript abundance and protein synthesis rates increased to 0.61 after 24 h to 0.65, confirming extensive post-transcriptional regulations (Fig. 6a-c). Most highly abundant mRNAs were translationally repressed and encoded ribosomal proteins (blue dots), translation initiation (green) and elongation factors (light green) (Fig. 6a,b). In total, the repressed transcripts constituted 52% of all mRNA molecules in naïve T cells (40,740 / 77,000). However, translation was not generally repressed in naïve T cells as illustrated by the two highly abundant mRNA species encoding ubiquitin and β_2M, which were both frequently translated (Fig. 6a,b).

To further investigate the post-transcriptional regulations underlying rapid T cell activation, we calculated the rate by which individual mRNAs were processed by ribosomes. The efficiency of mRNA translation was heterogeneous, with a median rate of 1.6 times min^{-1} in naïve T cells. 6 h following activation, the median rate by which a single mRNA molecule was read off, slightly increased to 2 times min^{-1}(Extended Data Fig. 5g). In general, these numbers agree well with previous studies in cell culture systems, in which translation

initiation was found to occur 1.5 – 2 times min^{-1} based on imaging of nascent polypeptide chains being synthetized from single mRNA molecules[29, 30, 31, 32].

Strikingly, we identified 242 mRNAs species that were strongly repressed in naïve T cells and more than three times faster translated 6 h after activation (Fig. 6d, Supplementary Table 5). For example, naïve T cells contained 67 copies of mRNAs encoding the early activation marker CD69, yet in our pulsed SILAC experiments active synthesis of CD69 proteins was never detected in naïve T cells (Fig. 6a). In contrast, 6 h after activation, the translation rate of CD69 increased from 0 to 598 proteins min^{-1} while the number of *CD69* mRNAs only increased 1.6-fold, from 67 to 111 copies. Thus, *CD69* transcripts were completely repressed in naïve T cells but 6 h after activation each mRNA was read off by ribosomes 5.4 times min^{-1} (mRNA translation rate, Fig. 6b). Consistent with a rapid onset of translation, total numbers of CD69 proteins increased from 0 copies in naïve T cells to 65,000 copies in 6 h-activated T cells (Fig. 6e). Similarly, mRNAs encoding the CD40L and JUN-B were completely silenced in naïve T cells but rapidly translated following activation, which led to a rapid increase in total protein copies (Figs. 6a,b, Extended Data Fig. 6a). Collectively, these findings illustrate a further example of preparedness whereby naïve T cells maintain a reservoir of repressed mRNAs that are rapidly engaged to initiate the activation program.

A majority of repressed mRNAs are regulated by mTOR

We next asked whether the rapid translational switch of repressed mRNAs in naïve T cells is regulated by mTOR signaling pathways, because the majority of repressed mRNAs contained a 5′-terminal oligopyrimidin (TOP) motif whose translation is regulated by mTORC1 in mouse embryonic fibroblasts[33]. To address this, we performed pulsed SILAC experiments with resting and 6 h-activated T cells that were treated with Torin-1,which inhibits mTORC1 and mTORC2 signaling pathways[34]. Consistent with low mTOR activity in naïve T cells[35], Torin-1 had a minimal effect on translation in naïve T cells (Fig. 6f). However, 6 h after activation Torin-1 strongly and specifically inhibited the translational switch of TOP mRNAs.

Interestingly,the activation-induced translational switch of 15 out of the 242 repressed mRNA species was not markedly affected by Torin-1 (Log_2 Fold change < 1). These included mRNA binding proteins RBMX, RBM3, and RBP39, as well as the early activation proteins CD69, NR4A1 (Nur77) and NR4A2 (Fig. 6g, Extended Data Fig. 6b). Thus, mTOR serves as a metabolic checkpoint controlling the translational switch for the majority of repressed mRNAs, yet a small subset including the fastest upregulated proteins were engaged independently of metabolic control.

Memory T cells have increased basal protein turnover

We next assessed translational dynamics in memory T cells, which sustain a higher metabolic activity and are more prepared to respond faster to antigens than naïve T cells[4, 8, 36]. Freshly isolated $CD45RO^+$ $CD4^+$ memory T cells from four healthy donors were labeled for 0, 6, 12, 24, and 48 h with heavy amino acids and their proteomes were analyzed by LC-MS. We found that the 23 proteins with highest turnover in naive T cells displayed comparable renewal kinetics in memory T cells (Fig. 7a and Extended Data Fig. 7a).

However, the global protein turnover rate was higher in memory T cells, with 100 proteins having significantly increased renewal rates at each time point ($P < 0.05$, two-tailed Welch's t test) (Supplementary Table 6). Of those, the strongest enriched KEGG annotations were *Ribosome* ($P_{adj} = 2.916\times10^{-11}$), *Glycolysis* ($P_{adj} = 2.356\times10^{-4}$) and *Proteasome* ($P_{adj} = 4.997\times10^{-3}$) (Fisher's exact test). For example, within 48 h ribosomal proteins RPS6 and RPL21 were renewed by ~25% in naïve T cells, which increased to ~50% in memory T cells (Fig. 7b). Similarly, renewal rates of glycolytic enzymes GAPDH and LDHA as well as proteasomal proteins PSMA1 and PSMA6 were approximately doubled in memory T cells (Fig. 7b). Thus, memory T cells are imprinted with high turnover of ribosomal, proteasomal and glycolytic proteins to support a higher state of preparedness.

With a total protein synthesis rate of ~110,000 proteins min^{-1} memory T cells had a translational output that was 80% higher than in naïve T cells (Fig. 7c). The average ribosomal output in resting memory T cells was ~1.47 amino acids sec^{-1} per ribosome,which was 93% higher than in naïve T cells. 6 h following activation the ribosomal output increased to ~4.3 amino acids sec^{-1} (Fig. 7d). Taken together, memory T cells have a higher baseline translational activity than naïve T cells and reach a higher ribosomal output early after initiation of the activation program,supporting a faster response.

Discussion

In this study we employed a pulsed SILAC approach to analyze the dynamics in protein synthesis and turnover in T cells. Our data revealed that naïve T cells are not entirely inert since they continuously replenish a small set of proteins that are either unstable or actively degraded. Thus, our analysis defines a minimal maintenance program that supports homeostasis of naïve T cells. For example, MHC-I-peptide complexes are unstable[37] and T cells continually replenish MHC-I molecules on their surface, which promotes the presentation of peptides. Another example of proteins that displayed high turnover were several TFs that actively maintain cell identity, quiescence and homeostasis. These TFs were likely rapidly renewed as a consequence of their usage[38]. These findings suggested that differential turnover rates of proteins support the execution of key cellular processes.

Our study also provides novel insights into mechanisms of T cell preparedness, enabling the rapid execution of their activation program. High turnover of specific proteins in resting T cells, while having high energy-costs, provides the advantage that protein abundance can be rapidly tuned down. Our analyses showed that a large number of proteins down regulated in response to different stimuli are of high turnover in the resting state, thus demonstrating high protein turnover is a process T cells employ to rapidly adjust their proteome for transitioning cell states.

A second mechanism of T cell preparedness is the maintenance of a reservoir of glycolytic enzymes, allowing naïve T cells to jump start glycolysis. Curiously, this reservoir was maintained in naïve T cells despite a lack of dependency on glycolysis as a metabolic program. However, T cells quickly engaged glycolysis following activation, and having a pre-existing reservoir of glycolytic enzymes facilitated this rapid switch. This finding also

explains how naïve T cells can temporally increase their glycolytic rate threefold within just a few minutes following stimulation[8].

A third mechanism of preparedness relies on a large pool of idling ribosomes,whose average translational output in naïve T cells increased from 0.8 to 4 aa/s within six hours following activation. Notably, the ribosomal output rates that we determined in activated T cells are in agreement with previously measured ribosome translocation rates of 3.1 – 5.6 aa/s based on translation imaging in live cells and ribosome profiling[31, 32, 39]. Thus, our data suggest that ribosomes idle in naïve T cells but operate at a high capacity in activated T cells.

Continuous transcription of untranslated mRNAs, which have a short half-life of about 7 h[40], comes at an energetic cost. Yet, sustaining the expression of repressed mRNAs has the advantage that they can be immediately engaged in protein synthesis. For example, naïve T cells contain several untranslated copies of mRNAs encoding CD69, which are immediately translated following activation to retain activated T cells in secondary lymphoid organs[41]. Globally, many of the mRNAs repressed in naïve T cells contained a TOP motif and were regulated by mTOR, linking metabolism to translational regulation in the T cell activation program. Most of these mRNAs encoded ribosomal proteins as well as transcription initiation and elongation factors. Consistent with our observations, previous studies showed that mRNAs encoding the translational machinery, although highly abundant, were barely associated with polysomes[6, 42, 43]. However, we also identified 15 repressed mRNAs that were rapidly engaged following activation independent of mTOR. Thus, there is a default, initial T cell activation program that is mTOR-independent and includes the upregulation of CD69 (to retain T cells in lymph nodes) and Nur77 (to regulate metabolism)[44].

Previous studies also demonstrated that naïve T cells are prepared to rapidly generate mRNAs as 90% of the promoters from genes to be expressed in activated T cells are loaded with polymerase[45]. Thus, naïve T cells also sustain a transcriptional preparedness level.

By combining absolute mRNA concentrations with quantifications of the transcriptome, we estimated mRNA copy numbers of each transcript in T cells. We found a total of ~77,000 and ~420,000 mRNA molecules in naïve and 24 h-activated T cells, respectively. Previously, RNA-Seq based estimates suggested that an average mammalian cell contains about 200,000 mRNAs molecules[46]. Our data showed that in naïve T cells proteins are about 5,000 times more abundant than transcripts and in 24 h-activated T cells about 3,000 times more abundant,indicating that translation is a crucial amplification step for the abundance of proteins in T cells.

Based on our pulsed SILAC data and protein quantifications, we estimated absolute synthesis rates for more than 1,300 proteins in T cells. Combined with estimations on mRNA copy numbers, we calculated that transcripts are on average processed 1.6 times per minute in naïve T cells and increased to 2 times per minute following activation. These data are in excellent agreement with previous observations of translation initiation frequencies in live cells, which occurred every 30 to 40 seconds on actively translated mRNAs[29, 30, 31, 32]. Thus, our global estimates of absolute protein synthesis rates and transcript abundances are both in accordance with previous studies in other cell types.

In conclusion, this study provides absolute numbers of mRNAs and protein copies as well as transcript processing and protein synthesis rates in T cells, which is an important resource for quantitative immunology. Our analysis of these datasets revealed a minimal maintenance and preparedness program in resting, human T cells.

Methods

Human primary T cells

Blood from healthy donors was obtained from the Swiss Blood Donation Center of Basel and Lugano, and used in compliance with the Federal Office of Public Health (authorization no. A000197/2 to F.S).Peripheral blood mononuclear cells (PBMCs) were isolated by Ficoll gradient centrifugation. $CD4^+$ T cells were enriched with magnetic microbeads (Miltenyi Biotec). Naive $CD4^+$ T cells were sorted as $CD4^+CD8^-CCR7^+CD45RA^+CD25^-$on a FACS Aria III cell sorter (BD Biosciences). For cell staining, the following antibodies were used: anti-CD4-APC (allophycocyanin), clone 13B8.2; anti-CD4-FITC (fluorescein isothiocyanate), clone 13B8.2; anti-CD8-APC, clone B9.11; anti-CD8-FITC, clone B9.11; anti-CD45RA-PE (phycoerythrin), clone alb11; anti-CD25-FITC, clone B1.49.9 (all from Beckman Coulter); anti-CCR7-Brilliant Violet 421, clone G043H7 (BioLegend).

Cell culture

Cells were cultured in RPMI-1640 medium supplemented with 2 mM glutamine, 1% (v/v) non-essential amino acids, 1% (v/v) sodium pyruvate, penicillin (50 U ml^{-1}), streptomycin (50 μg ml^{-1}; all from Invitrogen), and 5% (v/v) human serum (Swiss Blood Center, Basel). Human T cells were activated with plate-bound anti-CD3 (5 μg/ml, clone TR66) and anti-CD28 (1 μg/ml, clone CD28.2, BD Biosciences) for 48 h in 96-well Nunc Maxisorb plates. 1.5×10^5 T cells were plated per well. After 48 h of activation, cells were transferred to 96-well U-bottom plates and cultured in IL-2 containing media (500 U/ml). In experiments, in which T cells that were cultured without a stimulus, 1.5×10^5 T cells were plated in 96-well U-bottom plates and 200 μ1 of culture medium was added per well. Drugs were added at the following concentrations: CHX (50 μg/ml) and bortezomib/PS341 (10 μM).

For SILAC experiments, SILAC RPMI-1640 (GIBCO) was supplemented with 73 mg/l Lys-8 HCl and 42 mg/l Arg-10 HCl, 2 mM glutamine, 1% (v/v) sodium pyruvate, penicillin (50 U/ml), streptomycin (50 μg/ml; all from Invitrogen), and 5% (v/v) dialyzed human serum.

CRISPR/Cas9-mediated knockout of B2M

Lyophilized crRNAs targeting *B2M* (5′-CGUGAGUAAACCUGAAUCUUGUUUUAGAGCUAUGCU-3′, 5′-AAGUCAACUUCAAUGUCGGAGUUUUAGAGCUAUGCU-3′),CRISPR-Cas9 Negative Control crRNA (Alt-R® CRISPR-Cas9 Negative Control crRNA, cat # 1072544) and tracrRNA were chemically synthesized (IDT) and resuspended in Nuclease-Free Duplex Buffer at a stock concentration of 200 μM. To assemble Cas9-ribonucleotide proteins (RNPs), crRNAs and tracrRNAs were mixed at a 1:1 v/v ratio and incubated 5 min at 95°C to form duplexes at a final concentration of 44 μM. Next, Cas9 protein (Invitrogen,

ThermoFisher, 5 mg/mL stock) was added at a 1.5:1 v/v ratio (gRNA:Cas9) and incubated for 20 min at 21°C. Freshly isolated naive $CD4^+$ T cells were washed twice with PBS, re-suspended in Buffer T (Neon™ Transfection System Kit, cat #MPK1025) and mixed with the Cas9 RNP complex. Then, Cas9 Electroporation Enhancer (Alt-R® Cas9 Electroporation Enhancer, IDT, stock 10.8 μM) was added to the mix to a final concentration of 1.8 μM. A total of 1×10^6 cells was electroporated under the following conditions: voltage (2200 V), width (20 ms), pulse (one), 10 μL tip, Electrolytic Buffer E. Immediately after electroporation, cells were incubated at 37°C in 200 μL of pre-warmed media. After 24 h and 72 h post-transfection, cells were stained with an antibody to MHC-I (eBioscience, HLA-ABC-FITC, clone W6/32) and analyzed by flow cytometry.

Serial block-face scanning electron microscopy and 3D reconstruction

Human T cells were fixed in 2.5% glutaraldehyde (50 mM sodium cacodylate adjusted to pH 7.2, 50 mM KCl, 2.5 mM $CaCl_2$) for 60 min at 21°C[48]. Afterwards, the mixture was gently centrifuged (250 × g for 5 min), the supernatant was reduced, resuspended and introduced into cellulose capillary tubes[49] and sealed. After several rinses in cold buffer (50 mM sodium cacodylate pH 7.2), the specimens were immersed in freshly prepared reduced osmium mix (40 mM potassium ferrocyanide, 2% osmium tetroxide, 50 mM sodium cacodylate, 2 mM $MgCl_2$,) for 1 h at 4°C. Later, the samples were washed with deionized water at 21°C and immersed in 100 mM aqueous thiocarbohydrazide solution for 20 min at 21°C. Samples were then washed with deionized water and incubated in 2% osmium tetroxide for 30 min on ice. This was followed by overnight incubation in 0.5 % uranyl acetate on a rotating wheel at 4°C. Next, the samples were washed in deionised water and incubated in freshly prepared 20 mM lead aspartate solution for 30 min at 60°C. Samples were washed and dehydrated in graded ethanol series and propylene oxide, followed by embedding in epoxy resin and placed at 60°C for 48 h for polymerization. The final sample blocks were trimmed and glued to an aluminium SEM stub with conductive carbon cement (Ted Pella) to preserve conductivity and then placed in an incubator overnight at 37°C. Resin blocks were imaged by serial block face-scanning electron microscope (Quanta 200 FEG ESEM; FEI). To prevent charging artifacts, we used a chamber pressure of 0.32 Torr. The RAW images had a pixel size of 6.6 × 6.6 nm and were collected using a BSE detector at 4 kV accelerating voltage using digital micrograph software. The thickness of the slices was 100 nm. Image stacks were aligned using the TrackEM2 plugin for ImageJ[50]. Image analysis and quantification were performed using the IMOD software package[51].

Sample preparation for proteome analysis

Samples were processed as described by in[10]. Cell pellets were washed with PBS, lysed in 8M urea, 10 mM HEPES (pH 8), 10 mM DTT and then sonicated at 4°C for 15 min (level 5, Bioruptor, Diagenode). Alkylation was performed in the dark for 30 min by adding 55 mM iodoacetamide (IAA). A two-step proteolytic digestion was performed. First, samples were digested at 21°C (RT) with LysC (1:50, w/w) for 3 h. Then, they were diluted 1:5 with 50 mM ammonium bicarbonate (pH 8) and digested with trypsin (1:50, w/w) at 21°C overnight. The resulting peptide mixtures were acidified and loaded on C18 StageTips[52]. Peptides were eluted with 80% acetonitrile (ACN), dried using a SpeedVac centrifuge (Savant,

Concentrator plus, SC 110 A), and resuspended in 2% ACN, 0.1% trifluoroacetic acid (TFA), and 0.5% acetic acid.

LC-MS/MS for analysis of proteomes

Peptides were separated on an EASY-nLC 1200 HPLC system (Thermo Fisher Scientific) coupled online to a Q Exactive mass HF spectrometer via a nanoelectrospray source (Thermo Fisher Scientific)[53]. Peptides were loaded in buffer A (0.1% formic acid) on in house packed columns (75 μm inner diameter, 50 cm length, and 1.9 μm C18 particles from Dr. Maisch GmbH). Peptides were eluted with a non-linear 180 min gradient of 5%–60% buffer B (80% ACN, 0.1% formic acid) at a flow rate of 250 nl/min and a column temperature of 50°C. The Q Exactive was operated in a data dependent mode with a survey scan range of 300-1650 m/z and a resolution of 60,000 at m/z 200. Up to 10 most abundant isotope patterns with a charge ≥ 2 were isolated with a 1.8 Th wide isolation window and subjected to higher-energy C-trap dissociation (HCD) fragmentation at a normalized collision energy of 27. Fragmentation spectra were acquired with a resolution of 15,000 at m/z 200. Dynamic exclusion of sequenced peptides was set to 30 s to reduce the number of repeated sequences. Thresholds for the ion injection time and ion target values were set to 20 ms and 3E6 for the survey scans and 55 ms and 1E5 for the MS/MS scans, respectively. Data were acquired using the Xcalibur software (Thermo Scientific).

Analysis of proteomics data

MaxQuant software (version 1.5.3.54) was used to analyze MS raw files[54]. MS/MS spectra were searched against the human Uniprot FASTA database and a common contaminants database (247 entries) by the Andromeda search engine[55]. Cysteine carbamidomethylation was set as fixed and N-terminal acetylation and methionine oxidation as variable modification. Enzyme specificity was set to trypsin with a maximum of 2 missed cleavages and a minimum peptide length of 7 amino acids. A false discovery rate (FDR) of 1% was required for peptides and proteins. Peptide identification was performed with an allowed precursor mass deviation of up to 4.5 ppm and an allowed fragment mass deviation of 20 ppm. Nonlinear retention time alignment of all measured samples was performed in MaxQuant. Peptide identifications were matched across different replicates within a time window of 1 min of the aligned retention times. A minimum ratio count of 1 was required for valid quantification events via MaxQuant's Label Free Quantification algorithm (MaxLFQ). Data were filtered for common contaminants and peptides only identified by side modification were excluded from further analysis. Copy numbers were estimated based on the protein mass of cells[56]. We set the protein mass of a naive T cell to 25 pg and of an activated T cell to 75 pg.

Calculation of protein synthesis rates

Total protein copy numbers were estimated based on total LFQ values (heavy and light proteins). The number of newly synthesized protein copies was calculated based on the proportion of heavy proteins. For naïve T cells, the number of newly synthesized proteins within 6, 12, 24 and 48 h was analyzed and the highest rate (proteins/h) was selected.

RNA sequencing

Total RNA was isolated from flow sorted naïve $CD4^+$ T cells using the RNeasy Plus Mini Kit from Qiagen. RNA samples from two healthy donors were pooled and sent to IGA technology services. The TruSeq Stranded mRNA Sample Prep kit (Illumina) was used for library preparation starting with 1-2 μg of RNA (R.I.N. >7) as input. The poly-A mRNA was fragmented 3 min at 94°C and every purification step was performed by using 1X Agencourt AMPure XP beads. Both RNA samples and final libraries were quantified using the Qubit 2.0 Fluorometer (Invitrogen) and quality tested by Agilent 2100 Bioanalyzer RNA Nano assay (Agilent Technologies). Libraries were processed with Illumina cBot for cluster generation on the flowcell and sequenced on single-end mode at the multiplexing level requested on HiSeq2500 (Illumina). The CASAVA 1.8.2 version of the Illumina pipeline was used to process raw data for format conversion and de-multiplexing.

Estimation of absolute transcript copy numbers

To determine the total mRNA content per T cell, total RNA was isolated from naïve and activated T cells by using the E.Z.N.A. total RNA Kit I (Omega BIO-TEK). From total RNA, polyA-mRNA was isolated using polyT-coated dynabeads (dynabeads mRNA purification kit, Thermo Fischer Scientific). The amount of purified mRNA was quantified on a Qubit fluorometer (Thermo Fischer Scientific). The proportional mass (M_i) of each transcript was calculated using equation (1), where M_{mRNA} is the mass of total polyA-mRNA, $FPKM_i$ the FPKM value of each transcript determined by RNA-Seq and l_i the transcript length.

$$M_i = M_{mRNA} * \frac{FPKM_i * l_i}{\sum_{j=1}^{n} FPKM_j * l_j} \quad (1)$$

Copy numbers of each transcript (CN_i) were calculated using equation (2), where N_A is the Avogadro constant, $\overline{MW}$ the average molecular weight of a *ribonucleotide* monophosphate, and l_i the length of the transcript.

$$CN_i = M_i * \frac{N_A}{l_i * \overline{MW}} \quad (2)$$

ATAC sequencing

Accessible chromatin mapping was performed using the ATAC-seq method as previously described[1], with minor adaptations. In each experiment, 5×10^4 cells were centrifuged for 10 min at 8°C, resuspended in 50 μl ATAC-seq lysis buffer (10 mM Tris-HCl pH 7.4, 10 mM NaCl, 3 mM $MgCl_2$ and 0.1% NP-40) and centrifuged for 30 min at 500g and 8 °C. After centrifugation, the pellet was incubated in 25 μl transposase reaction mix (12.5 μl 2x TD buffer, 1 μl transposase (Illumina) and 11.5 μl nuclease-free water) for 60 min at 37 °C. After DNA purification with the Clean and Concentrator kit (Zymoresearch), 50 μl PCR reaction was setup (10 μl transposed DNA, 10 μl nuclease-free H_2O, 2.5 μl PCR primer 1, 2.5 μl barcoded PCR primer 2 and 25 μl kNEBNext Ultra II Q5 master mix (New England Biolabs Inc.). After 5 cycles, 5 μl of the eluted DNA was used in a quantitative PCR (qPCR)

reaction to estimate the optimum number of amplification cycles. Remaining 45 μl were amplified for the determined cycle number. Library amplification was followed by 2 rounds of AMPure XP bead (Agencourt) size selection to exclude fragments larger than 1,200 bp. DNA concentration was measured with a Qubit fluorometer (Life Technologies). The libraries were sequenced by the Genomic Core Sequencing Facility at EMBL using the Illumina HiSeq2500 platform and the 50-bp single-end configuration.

Processing of the ATAC-seq data

Reads were aligned to the GRCh38/hg38 assembly of the human genome using Bowtie with the '--best and -m 1' parameters to eliminate strand bias and report only best alignment in terms of quality values at mismatched position and to allow only one (depending on quality value) alignment per read, respectively. All downstream analyses were performed on the filtered reads. Greater than 100 million reads were obtained for the library, and reads mapping to mitochondrial DNA were excluded from the analysis. Between 22, 4 million and 27, 6 million high-quality reads per sample that mapped uniquely to genomic DNA were retained. Peaks were called for each sample using HOMER with parameters '-style factor and -L 20', to analyze transcription factors and call peaks with 20-fold greater tag density than in the surrounding 10kb region, respectively. Differential peaks were identified using 'getDifferentialPeaksreplicates.pl -balanced –edgeR (statistical program) -L 10 (10-fold greater tag density than background)'. Peaks were merged for the same cell type using mergePeaks and annotated with annotatePeaks.pl. One non-annotated file was generated with the option "-noann', uploaded to Rstudio and with the package ggplot2 principal component analysis was performed. Motif analysis on peak regions was performed by HOMER function findMotifsGenome.pl with the parameters '-size 200 (peak size) and -len 8,10,12,15 (motif length)'. With the '-size 200 -hist 400 (bin size in bp) -ghist (outputs gene profiles for each gene)'-parameters from HOMER a data matrix file was generated and uploaded to Cluster 3.0 for clustering (parameters: normalize genes, cluster genes and array, similarity metric: correlated uncentered) and visualized with Java Tree View.

ChIP sequencing

ChIP was performed as previously described[57]. In brief, 50×10^6 $CD4^+$ T cells, pooled from three different healthy donors, were fixed in 1% formaldehyde (Sigma-Aldrich) for exactly 10 min at 20 °C under rotation. The crosslinking reaction was quenched by the addition of 125 mM Tris-HCl, pH 7.6, for 5 min at 20°C. Cells were washed three times with ice-cold PBS. The cell pellet was then resuspended in 1.5 ml RIPA buffer (without Triton X-100) supplemented with protease inhibitors (Halt Protease Inhibitor Cocktail, Thermo Scientific) and was frozen at −80°C. After thawing, chromatin was sheared with a Bioruptor Plus bath sonicator (Diagenode) with the following settings: ten cycles of 30 s "on" and 60 s "off", five times (50 cycles in total), at high intensity and 4°C. Every ten cycles, samples were briefly vortexed and spun down. The shearing of DNA into 200- to 300-bp fragments was evaluated by electrophoresis through a 1.5% agarose gel. Before the immunoprecipitation, 1% Triton X-100 was added to the sample, and an aliquot was stored at –20°C as input control. Antibody-bound Protein G Dynabeads (Life Technologies) were added to each sample, and immunoprecipitation was performed overnight at 4°C on a rotating wheel. 10 μg of ChIP-grade anti-ETS-1 antibody (Santa Cruz Biotechnology, cat. num. sc-350 X, clone

Europe PMC Funders Author Manuscripts

C-20) was used for the immunoprecipitation. The next day, the Dynabeads were thoroughly washed, and the eluted DNA was subjected to RNAse A and proteinase K treatments before overnight de-crosslinking at 65 °C. Finally, de-crosslinked DNA was purified with SPRI magnetic beads and was eluted in 10 mM Tris-Cl, pH 8.0. ChIP DNA was quantified with the dsDNA HS assay kit (Life Technologies, cat. num. Q32854) on a Qubit 2.0 device. ChIP-seq libraries were prepared as previously described [57]. Illumina-compatible universal and indexed adapters and amplification primers were synthesized by Microsynth AG. Sequencing was performed on an Illumina HiSeq platform. About 25 million reads and 50 million reads (each unique single-end 50 bp reads) were generated for the ChIP sample and the input sample, respectively.

ChIP-seq data were analyzed with the Fish the ChIP's automated genomic annotation tool[58]. Enriched DNA motifs in the ETS-1 ChIP-seq dataset were identified by MEME-ChIP (v.5.1)[59]. ETS-1 peaks were assigned by proximity to the neighboring genes using the GREAT (v.3 or later) web-based software[60].

Statistical Analysis

Statistical analyses were performed in the R programming environment (version 3.3.3) or with GraphPad Prism 7 (GraphPad Software).

Extended Data

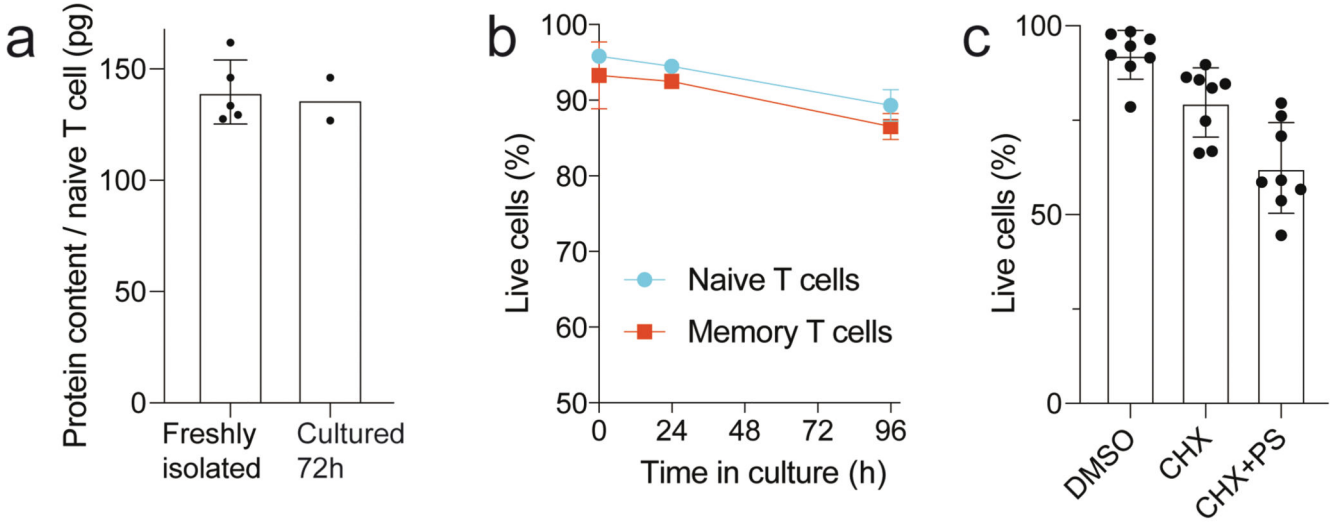

Extended Data Fig. 1. Viability of resting T cells in culture.

(a) Protein mass of naïve T cells does not change after 72h of culturing. Proteomes of T cells that were either analyzed immediately after isolation or after 72h of culturing were analyzed by LC-MS. Protein content was estimated using the proteome ruler approach[47]. n=5 for freshly isolated and n= 2 for 72h-cultured T cells from different donors. Bars represent the S.E.M **(b)** FACS-purified naïve and memory T cells were cultured in complete medium without the addition of growth factors. To measure cell viability, T cells were stained with Annexin-V-FITC directly after sorting or after 24h and 96h of culturing and

then analyzed by flow cytometry. n=4, Four independent experiments with T cells from two different donors. Bars represent the S.E.M. **(c)** FACS-purified naïve T cells were cultured for 24h in complete medium containing either DMSO, 50 μg/ml CHX or 50 μg/ml CHX together with 10 μM bortezomib (CHX + PS). n=8 from three different donors. Bars represent the S.E.M

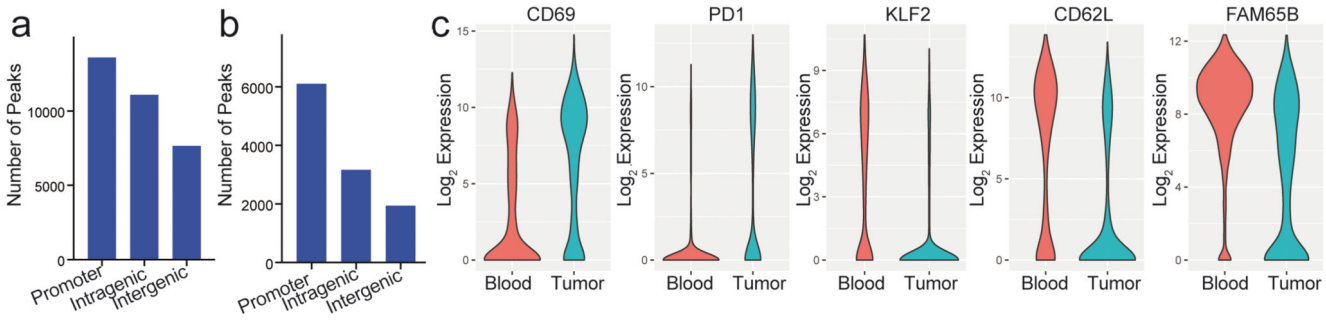

Extended Data Fig. 2. Analysis of hallmark transcription factors.

(a) Frequency of ATAC-Seq peaksannotated to different genomic regions. **(b)** Frequency of ETS1 ChIP-Seq peaksannotated to different genomic regions. **(c)** Examples of activation markers that were up-regulated in TILs (CD69 and PD1) and proteins that were downregulated (KLF2, CD62L, and FAM65B). n=1627 for T cells from blood, n=2170 for T cells from tumors. Violin plot width is based on a Gaussian kernel density estimate of the data (estimated by the density function with standard parameters), scaled to have maximum width = 1. Data are from Zheng et al. 2016.

Europe PMC Funders Author Manuscripts

Europe PMC Funders Author Manuscripts

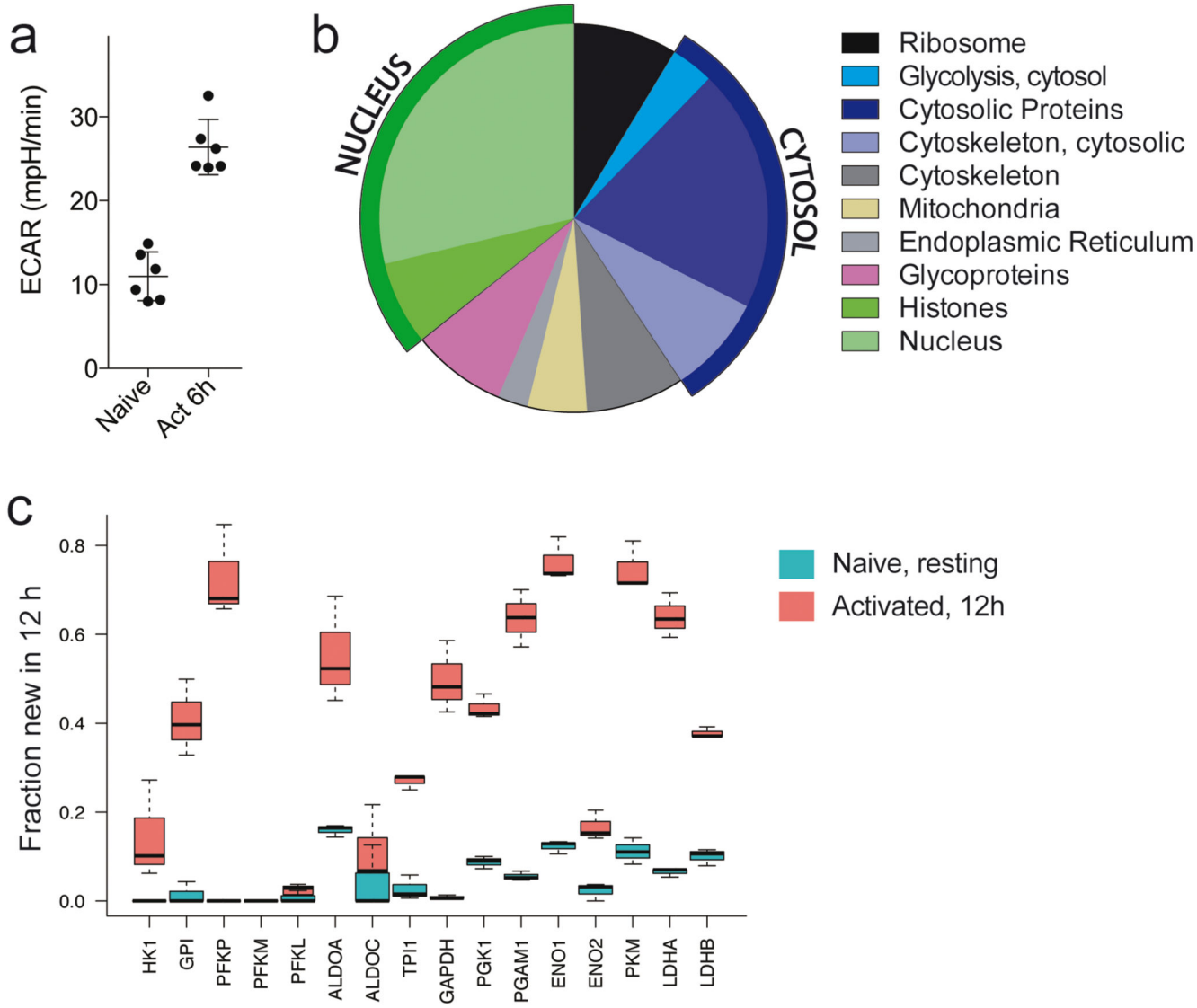

Extended Data Fig. 3. Increased turnover of glycolytic enzymes following activation.

(a) Naïve or 6h-activated T cells were analyzed on a Seahorse analyzer. Shown is the Extra Cellular Acidification Rate (ECAR), which is a measure of the glycolytic rate. n=6 from three donors. Bars represent the S.E.M **(b)** Gene ontology analysis of the proteome of naïve T cells. Glycolytic proteins (blue) contributed 11% to the cytosolic protein mass. **(c)** Fraction of newly synthetized (heavily labeled) glycolytic proteins after a 12-hours pulse in naïve or 12h-activated T cells. n=3 from three different donors. Box plot elements are defined as in Fig. 2b

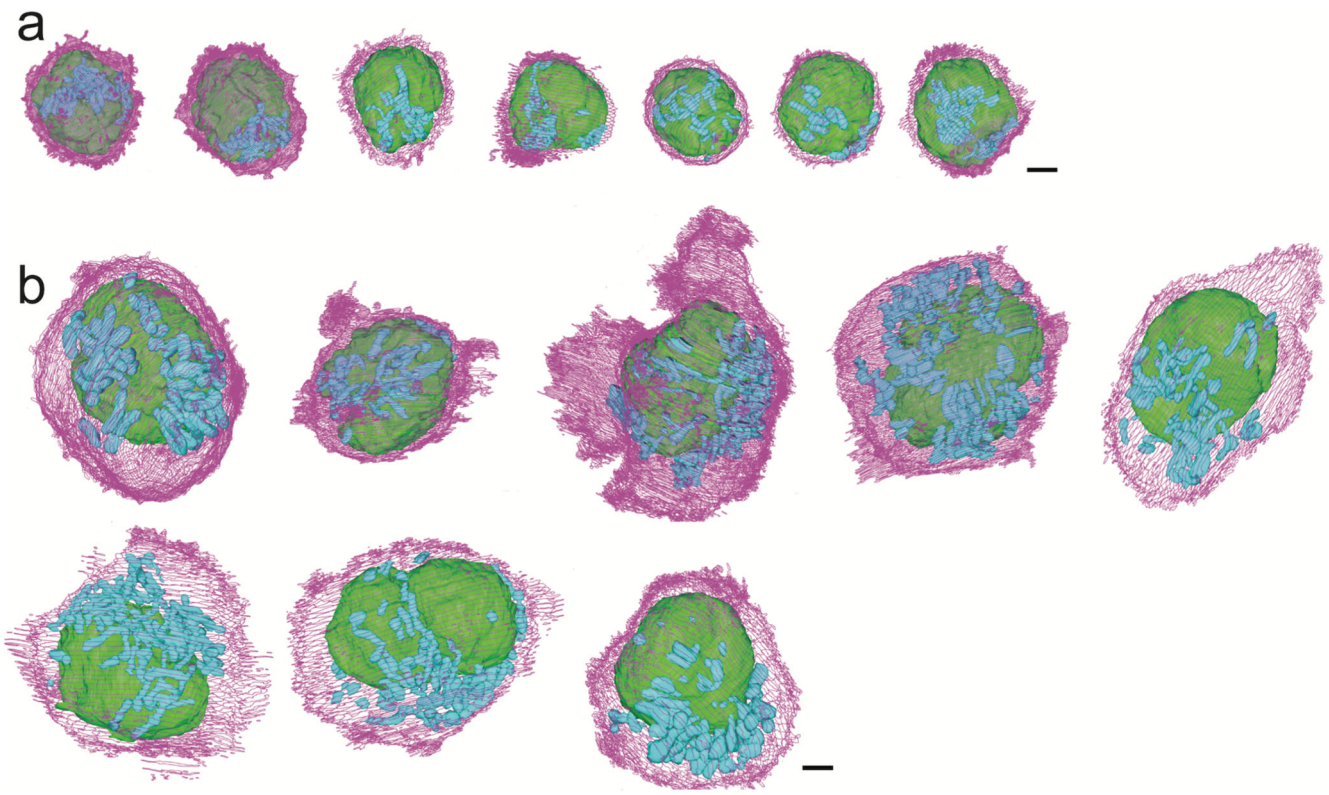

Extended Data Fig. 4. 3D reconstructions of seven naïve and eight 72 h-activated T cells.
(a) Reconstructions of naïve $CD4^+$ T cells. For the first two cells every layer of the plasma membrane (purple) was drawn, while for the other cells only every third layer was drawn. Scale bar = 2 μm **(b)** Reconstructions of 72 h-activated $CD4^+$ T cells. For the first four cells every layer of the plasma membrane (purple) was drawn, while for the other cells only every third layer was drawn. Scale bar = 2 μm

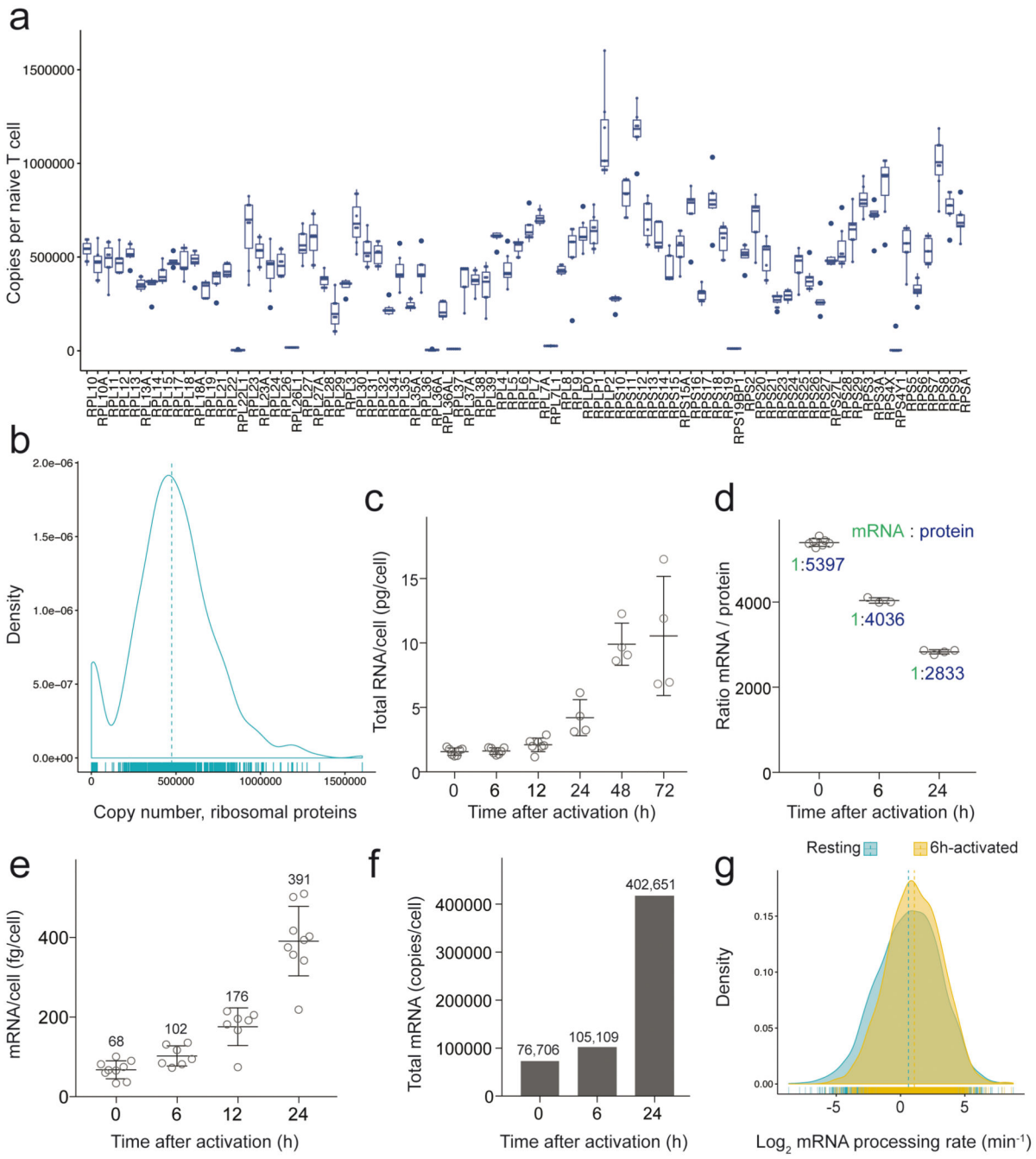

Extended Data Fig. 5. Estimation of the number of ribosomes.

(a) Copy numbers of 82 ribosomal proteins in naïve T cells. n=7 from seven different donors. Box plot elements are defined as in Fig. 2b **(b)** Distribution of the copy numbers of ribosomal proteins in naïve T cells. Average values from n=7 are shown. Dashed line shows the median, which was used as an approximation of total ribosomes. **(c)** Total RNA in naïve and activated T cells. To estimate the number of ribosomes, it was assumed that 83% of total RNA was ribosomal RNA. n=7 for naïve, 6h and 12h-activated T cells. n=4 for 24h, 48h and 72h activated T cells from different donors. Bars represent the S.E.M **(d)** mRNA to protein

ratio. n=7 for naïve, n=3 for 6h and n=4 for 24h activated T cells from different donors. Bars represent the S.E.M **(e)** Total amount of mRNA per T cell. n=9 for naïve and 24h activated T cells,n=7 for 6h and 12h activated T cells from different donors. Bars represent the S.E.M **(f)** Average mRNA copy numbers per T cell. **(g)** mRNA processing rate in naïve and 6h-activated T cells. Average values from n=3 from different donors are shown.

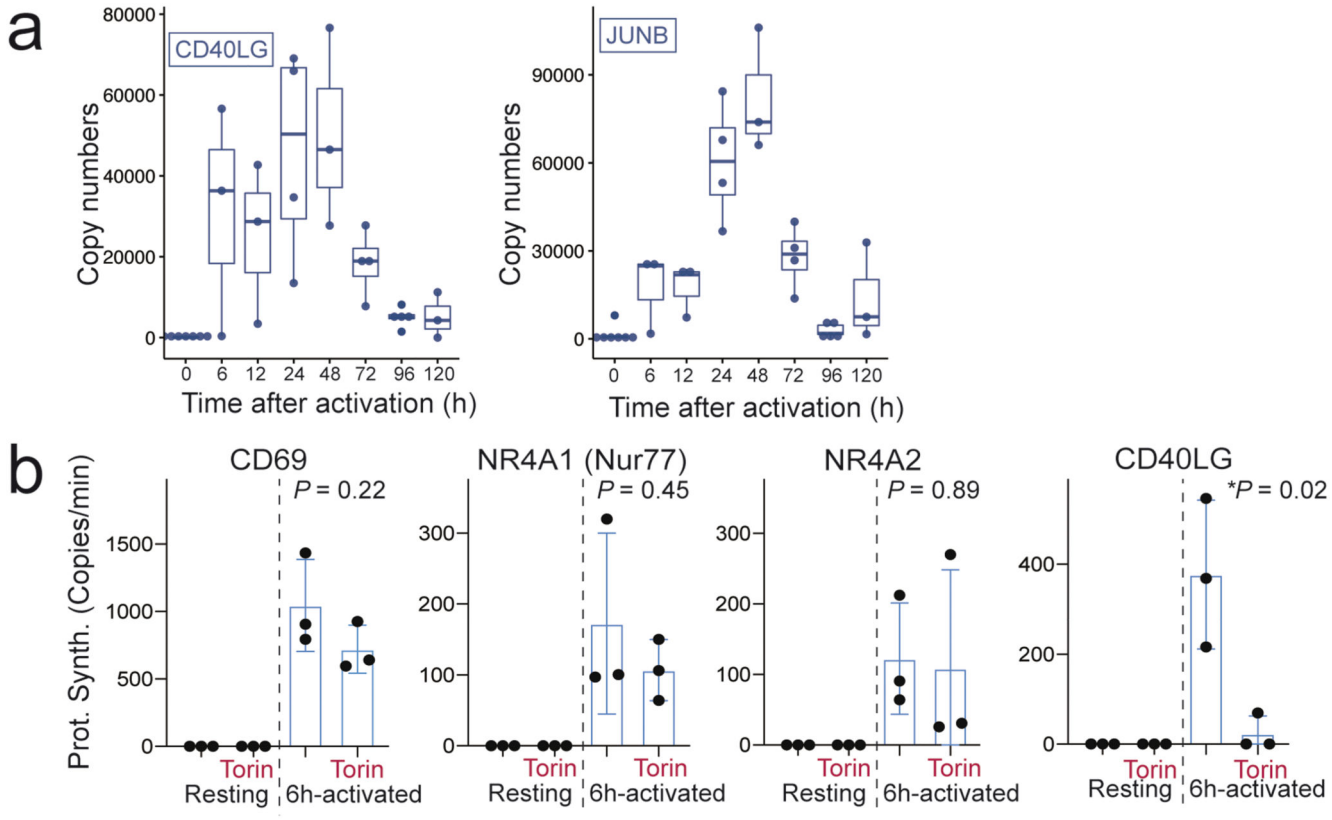

Extended Data Fig. 6. Posttranscriptional regulations.

(a) Absolute copy numbers of CD40LG and JUNB proteins in resting and activated T cells.n=7 for naïve T cells, n=3 for 6h, 12h, 48h, 120h-activated T cells, n=4 for 24h, 72h, 96h activated T cells. Box plot elements are defined as in Fig. 2b **(b)** Absolute protein synthesis rates in resting and 6h-activated T cells that were untreated or treated with Torin-1. n=3 from three donors. Bars represent the S.E.M.

Europe PMC Funders Author Manuscripts

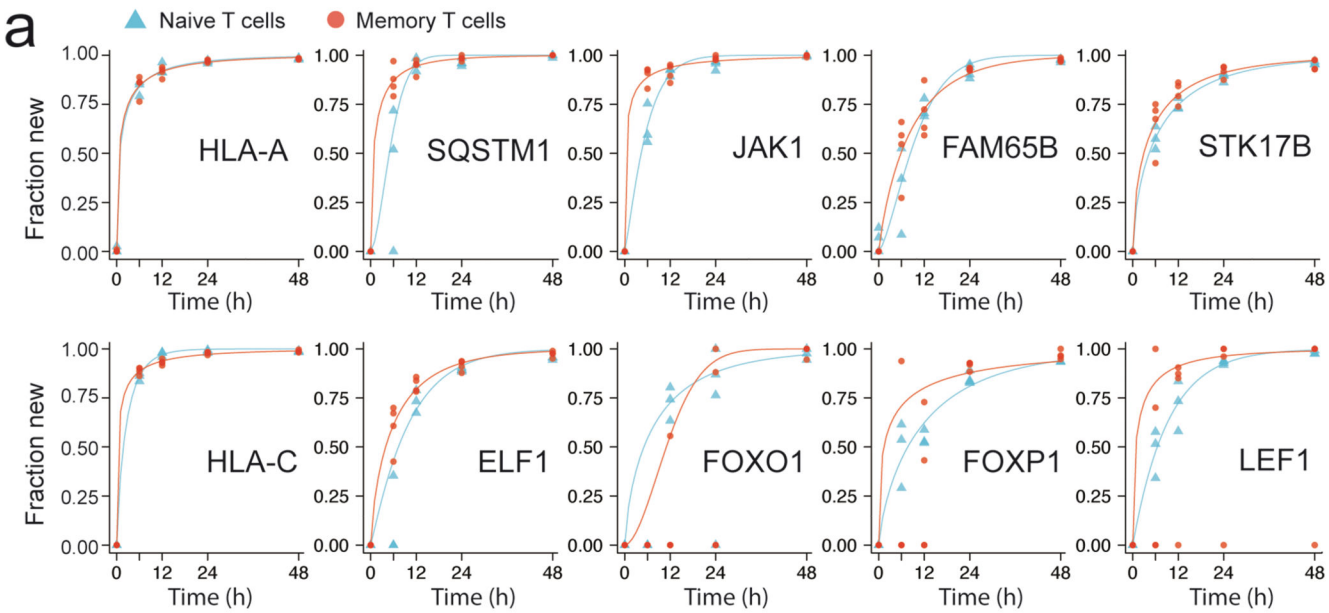

Extended Data Fig. 7. Rapidly turned over proteins in naïve and memory T cells.

(a) Comparison of protein turnover kinetics in resting naïve and memory $CD4^+$ T cells of selected proteins. n=3 for naïve 6h andnaïve 12h; n=4 for naïve 24h, memory 6h, memory 12h andmemory 24hfrom different donors.

Supplementary Material

Refer to Web version on PubMed Central for supplementary material.

Acknowledgements

We thank D.Jarrossay for cell sorting. This work was supported by a grant from the Swiss SystemsX.ch initiative, evaluated by the Swiss National Science Foundation (grant no 142032 to R.G.), the European Research Council (grant no 803150 to R.G.), the Swiss National Science Foundation (grant no 170213 to F.S.), the Federal Ministry of Education and Research (GAIN_01GM1910A to B.G.) and the German Research Foundation (SFB1160/2_B5, RESIST–EXC 2155–Project ID 39087428 to B.G).The Institute for Research in Biomedicine is supported by the Helmut Horten Foundation.

Data Availability

The mass spectrometry proteomics raw data have been deposited to the ProteomeXchange Consortium via the PRIDE [1] partner repository with the dataset identifier PXD017159.RNA-seq and ChIP-seq have been deposited to the NCBI Gene Expression Omnibus (GEO) with the accession number GSE147229 and GSE146787. The data that support the findings of this study are available at www.immunomics.ch or are attached as supplementary tables or are available from the corresponding author upon request.

References

1. Crabtree GR. Contingent genetic regulatory events in T lymphocyte activation. Science. 1989; 243:355–361. [PubMed: 2783497]

2. Vrisekoop N, et al. Sparse production but preferential incorporation of recently produced naive T cells in the human peripheral pool. Proceedings of the National Academy of Sciences of the United States of America. 2008; 105:6115–6120. [PubMed: 18420820]
3. Chapman NM, Boothby MR, Chi H. Metabolic coordination of T cell quiescence and activation. Nature reviews Immunology. 2019
4. Pearce EL, Poffenberger MC, Chang C-H, Jones RG. Fueling immunity: insights into metabolism and lymphocyte function. Science. 2013; 342:1242454. [PubMed: 24115444]
5. Fox CJ, Hammerman PS, Thompson CB. Fuel feeds function: energy metabolism and the T-cell response. Nature reviews Immunology. 2005; 5:844–852.
6. Araki K, et al. Translation is actively regulated during the differentiation of CD8+ effector T cells. Nature immunology. 2017; 18:1046. [PubMed: 28714979]
7. Sinclair LV, et al. Control of amino-acid transport by antigen receptors coordinates the metabolic reprogramming essential for T cell differentiation. Nature immunology. 2013; 14:500–508. [PubMed: 23525088]
8. Gubser PM, et al. Rapid effector function of memory CD8+ T cells requires an immediate-early glycolytic switch. Nature immunology. 2013; 14:1064–1072. [PubMed: 23955661]
9. Buck MD, Sowell RT, Kaech SM, Pearce EL. Metabolic instruction of immunity. Cell. 2017; 169:570–586. [PubMed: 28475890]
10. Geiger R, et al. L-Arginine Modulates T Cell Metabolism and Enhances Survival and Anti-tumor Activity. Cell. 2016; 167:829–842 e813. [PubMed: 27745970]
11. Howden AJ, et al. Quantitative analysis of T cell proteomes and environmental sensors during T cell differentiation. Nature immunology. 2019:1–13.
12. Ron-Harel N, et al. Mitochondrial biogenesis and proteome remodeling promote one-carbon metabolism for T cell activation. Cell metabolism. 2016; 24:104–117. [PubMed: 27411012]
13. Kaech SM, Hemby S, Kersh E, Ahmed R. Molecular and functional profiling of memory CD8 T cell differentiation. Cell. 2002; 111:837–851. [PubMed: 12526810]
14. Phan AT, Goldrath AW, Glass CK. Metabolic and epigenetic coordination of T cell and macrophage immunity. Immunity. 2017; 46:714–729. [PubMed: 28514673]
15. Schwanhäusser B, et al. Global quantification of mammalian gene expression control. Nature. 2011; 473:337–342. [PubMed: 21593866]
16. Ong S-E, et al. Stable isotope labeling by amino acids in cell culture, SILAC, as a simple and accurate approach to expression proteomics. Molecular & cellular proteomics. 2002; 1:376–386. [PubMed: 12118079]
17. Jovanovic M, et al. Dynamic profiling of the protein life cycle in response to pathogens. Science. 2015; 347:1259038. [PubMed: 25745177]
18. Aebersold R, Mann M. Mass-spectrometric exploration of proteome structure and function. Nature. 2016; 537:347–355. [PubMed: 27629641]
19. Wiśniewski JR, et al. Extensive quantitative remodeling of the proteome between normal colon tissue and adenocarcinoma. Molecular systems biology. 2012; 8:611. [PubMed: 22968445]
20. Bjørkøy G, et al. p62/SQSTM1 forms protein aggregates degraded by autophagy and has a protective effect on huntingtin-induced cell death. The Journal of cell biology. 2005; 171:603–614. [PubMed: 16286508]
21. Wu N, et al. AMPK-dependent degradation of TXNIP upon energy stress leads to enhanced glucose uptake via GLUT1. Molecular cell. 2013; 49:1167–1175. [PubMed: 23453806]
22. Weinreich MA, et al. KLF2 transcription-factor deficiency in T cells results in unrestrained cytokine production and upregulation of bystander chemokine receptors. Immunity. 2009; 31:122–130. [PubMed: 19592277]
23. Muthusamy N, Barton K, Leiden JM. Defective activation and survival of T cells lacking the Ets-1 transcription factor. Nature. 1995; 377:639. [PubMed: 7566177]
24. Bories J-C, et al. Increased T-cell apoptosis and terminal B-cell differentiation induced by inactivation of the Ets-1 proto-oncogene. Nature. 1995; 377:635. [PubMed: 7566176]

25. Buenrostro JD, Giresi PG, Zaba LC, Chang HY, Greenleaf WJ. Transposition of native chromatin for fast and sensitive epigenomic profiling of open chromatin, DNA-binding proteins and nucleosome position. Nature methods. 2013; 10:1213. [PubMed: 24097267]
26. Froehlich J, et al. FAM65B controls the proliferation of transformed and primary T cells. Oncotarget. 2016; 7:63215. [PubMed: 27556504]
27. Binnewies M, et al. Understanding the tumor immune microenvironment (TIME) for effective therapy. Nature medicine. 2018; 24:541.
28. Zheng C, et al. Landscape of infiltrating T cells in liver cancer revealed by single-cell sequencing. Cell. 2017; 169:1342–1356. e1316. [PubMed: 28622514]
29. Morisaki T, et al. Real-time quantification of single RNA translation dynamics in living cells. Science. 2016; 352:1425–1429. [PubMed: 27313040]
30. Wu B, Eliscovich C, Yoon YJ, Singer RH. Translation dynamics of single mRNAs in live cells and neurons. Science. 2016; 352:1430–1435. [PubMed: 27313041]
31. Yan X, Hoek TA, Vale RD, Tanenbaum ME. Dynamics of translation of single mRNA molecules in vivo. Cell. 2016; 165:976–989. [PubMed: 27153498]
32. Wang C, Han B, Zhou R, Zhuang X. Real-time imaging of translation on single mRNA transcripts in live cells. Cell. 2016; 165:990–1001. [PubMed: 27153499]
33. Thoreen CC, et al. A unifying model for mTORC1-mediated regulation of mRNA translation. Nature. 2012; 485:109. [PubMed: 22552098]
34. Thoreen CC, et al. An ATP-competitive mammalian target of rapamycin inhibitor reveals rapamycin-resistant functions of mTORC1. Journal of Biological Chemistry. 2009; 284:8023–8032.
35. Yang K, Neale G, Green DR, He W, Chi H. The tumor suppressor Tsc1 enforces quiescence of naive T cells to promote immune homeostasis and function. Nature immunology. 2011; 12:888. [PubMed: 21765414]
36. Iezzi G, Karjalainen K, Lanzavecchia A. The duration of antigenic stimulation determines the fate of naive and effector T cells. Immunity. 1998; 8:89–95. [PubMed: 9462514]
37. Harndahl M, Rasmussen M, Roder G, Buus S. Real-time, high-throughput measurements of peptide–MHC-I dissociation using a scintillation proximity assay. Journal of immunological methods. 2011; 374:5–12. [PubMed: 21044632]
38. Lipford JR, Deshaies RJ. Diverse roles for ubiquitin-dependent proteolysis in transcriptional activation. Nature cell biology. 2003; 5:845–850. [PubMed: 14523392]
39. Ingolia NT, Lareau LF, Weissman JS. Ribosome profiling of mouse embryonic stem cells reveals the complexity and dynamics of mammalian proteomes. Cell. 2011; 147:789–802. [PubMed: 22056041]
40. Sharova LV, et al. Database for mRNA half-life of 19 977 genes obtained by DNA microarray analysis of pluripotent and differentiating mouse embryonic stem cells. DNA research. 2008; 16:45–58. [PubMed: 19001483]
41. Shiow LR, et al. CD69 acts downstream of interferon-α/β to inhibit S1P1 and lymphocyte egress from lymphoid organs. Nature. 2006; 440:540–544. [PubMed: 16525420]
42. Ricciardi S, et al. The Translational Machinery of Human CD4(+) T Cells Is Poised for Activation and Controls the Switch from Quiescence to Metabolic Remodeling. Cell metabolism. 2018; 28:961. [PubMed: 30517897]
43. Tan TC, et al. Suboptimal T-cell receptor signaling compromises protein translation, ribosome biogenesis, and proliferation of mouse CD8 T cells. Proceedings of the National Academy of Sciences. 2017; 114:E6117–E6126.
44. Liebmann M, et al. Nur77 serves as a molecular brake of the metabolic switch during T cell activation to restrict autoimmunity. Proceedings of the National Academy of Sciences. 2018; 115:E8017–E8026.
45. Kouzine F, et al. Global regulation of promoter melting in naive lymphocytes. Cell. 2013; 153:988–999. [PubMed: 23706737]
46. Shapiro E, Biezuner T, Linnarsson S. Single-cell sequencing-based technologies will revolutionize whole-organism science. Nature Reviews Genetics. 2013; 14:618.

47. Wiśniewski JR, Hein MY, Cox J, Mann M. A “proteomic ruler” for protein copy number and concentration estimation without spike-in standards. Molecular & cellular proteomics. 2014; 13:3497–3506. [PubMed: 25225357]
48. Akat K, et al. Molecular characterization of desmosomes in meningiomas and arachnoidal tissue. Acta neuropathologica. 2003; 106:337–347. [PubMed: 12845453]
49. Hohenberg H, Mannweiler K, Müller M. High-pressure freezing of cell suspensions in cellulose capillary tubes. Journal of microscopy. 1994; 175:34–43. [PubMed: 7932676]
50. Cardona A, et al. An integrated micro-and macroarchitectural analysis of the Drosophila brain by computer-assisted serial section electron microscopy. PLoS biology. 2010; 8:e1000502. [PubMed: 20957184]
51. Kremer JR, Mastronarde DN, McIntosh JR. Computer visualization of three-dimensional image data using IMOD. Journal of structural biology. 1996; 116:71–76. [PubMed: 8742726]
52. Rappsilber J, Mann M, Ishihama Y. Protocol for micro-purification, enrichment, pre-fractionation and storage of peptides for proteomics using StageTips. Nature protocols. 2007; 2:1896–1906. [PubMed: 17703201]
53. Scheltema RA, et al. The Q Exactive HF, a Benchtop mass spectrometer with a pre-filter, high-performance quadrupole and an ultra-high-field Orbitrap analyzer. Molecular & cellular proteomics : MCP. 2014; 13:3698–3708. [PubMed: 25360005]
54. Cox J, Mann M. MaxQuant enables high peptide identification rates, individualized p.p.b.-range mass accuracies and proteome-wide protein quantification. Nature biotechnology. 2008; 26:1367–1372.
55. Cox J, et al. Andromeda: a peptide search engine integrated into the MaxQuant environment. Journal of proteome research. 2011; 10:1794–1805. [PubMed: 21254760]
56. Wisniewski JR, et al. Extensive quantitative remodeling of the proteome between normal colon tissue and adenocarcinoma. Molecular systems biology. 2012; 8:611. [PubMed: 22968445]
57. Blecher-Gonen R, et al. High-throughput chromatin immunoprecipitation for genome-wide mapping of in vivo protein-DNA interactions and epigenomic states. Nat Protoc. 2013; 8:539–554. [PubMed: 23429716]
58. Barozzi I, Termanini A, Minucci S, Natoli G. Fish the ChIPs: a pipeline for automated genomic annotation of ChIP-Seq data. Biol Direct. 2011; 6:51. [PubMed: 21978789]
59. Machanick P, Bailey TL. MEME-ChIP: motif analysis of large DNA datasets. Bioinformatics. 2011; 27:1696–1697. [PubMed: 21486936]
60. McLean CY, et al. GREAT improves functional interpretation of cis-regulatory regions. Nat Biotechnol. 2010; 28:495–501. [PubMed: 20436461]

Europe PMC Funders Author Manuscripts

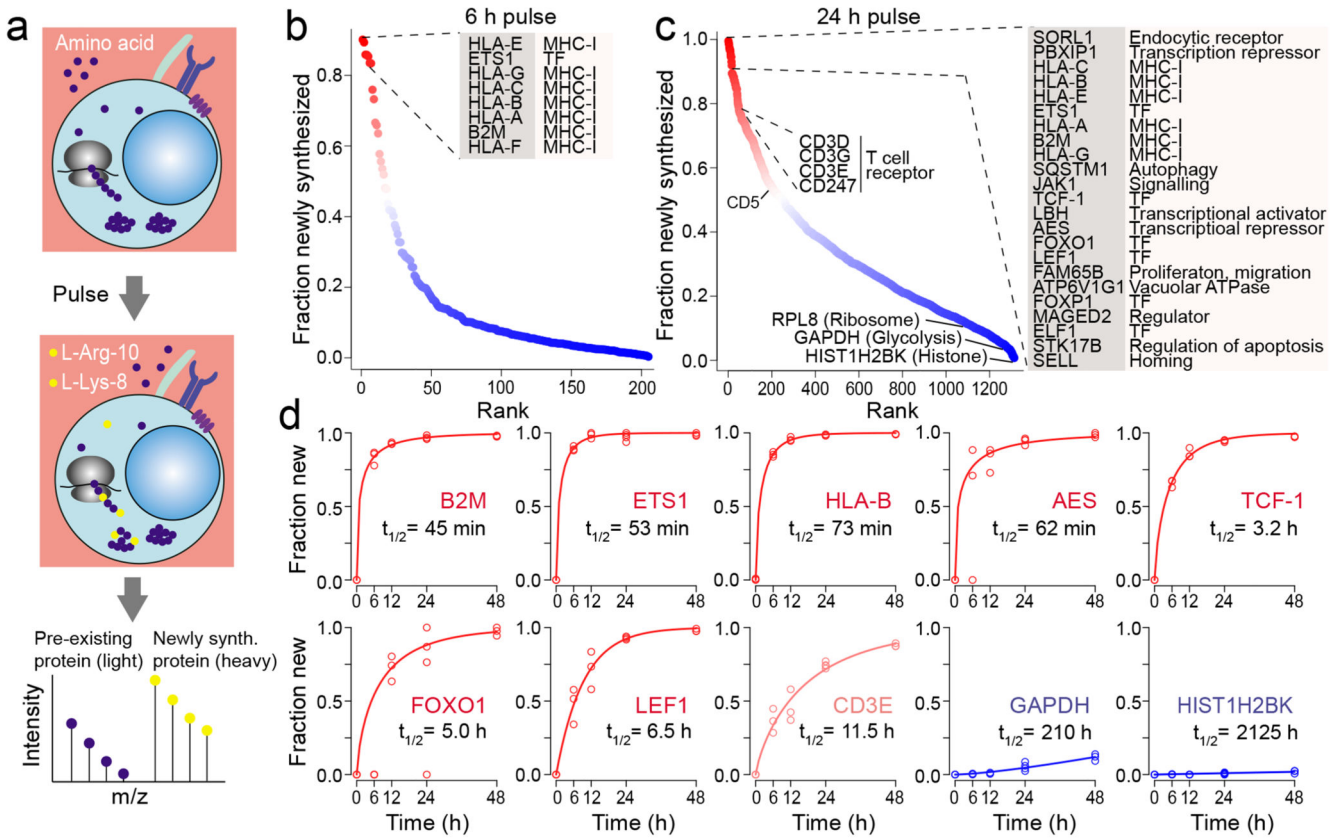

Fig. 1. A pulsed SILACapproach shows that a small set of important proteins is rapidly renewed in naïve T cells.

(a) Schematic of the pulsed SILAC workflow. **(b)** Shown are 205 protein species, which incorporated heavy amino acids after a 6 h pulse, ranked according to the fraction that was newly synthetized within 6 h. Average values from n=3 are shown. The inset shows protein species that were renewed by more than 80% in 6 h. Dots are colored according to turnover rate (Red to blue; Fast to slow) **(c)** Shown are1,313 protein species, which incorporated heavy amino acids after a 24 h pulse, ranked according to the fraction that was newly synthetized within 24h. Average values from n=3 are shown. The first inset shows protein species that were renewed by more than 90% in 24 h. A second inset shows components of the TCR. **(d)** Renewal kinetics of selected proteins. The half time ($t_{1/2}$) was calculated by fitting a cumulative Weibull distribution. n=3 from three different donors.

Europe PMC Funders Author Manuscripts

Europe PMC Funders Author Manuscripts

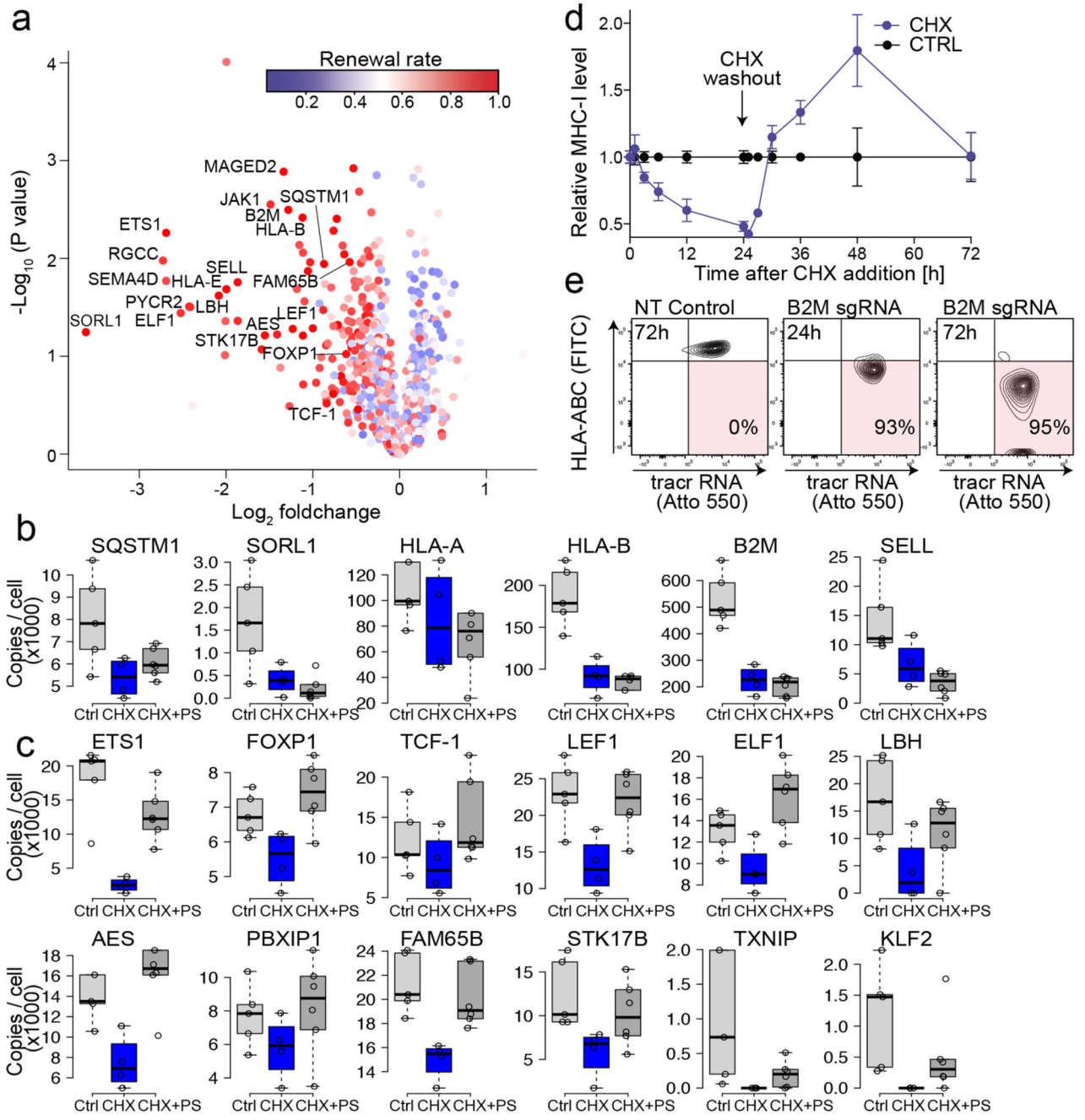

Fig. 2. Constitutive protein degradation in naïve T cells

(a) Naïve CD4$^+$ T cells were cultured in the presence or absence of 50 μg/ml cycloheximide (CHX) for 24 h, after which their proteomes were analyzed by mass spectrometry. Volcano plot fromdifferential abundance analysis (two-tailed Welch's t test) between control and CHX-treated cells. Each dot represents a protein; a negative Log2 foldchange means that the protein is less abundant in CHX-treated T cells. Only the 1,313 proteins shown in Fig. 1C, for which a renewal rate was also determined, are shown. The color code shows the renewal rate as determined by pulsed SILAC. n=4 from four different donors. **(b)** Naïve CD4$^+$ T

cells were treated with 50 μg/ml CHX alone or together with 10 μM bortezomib/PS341 (PS). Boxplot shows copy numbers of selected membrane proteins. n=5 for Ctrls, n=4 for CHX, n=6 for CHX+PS. Box plots denote the medians and the IQRs. The whiskers of each box plot are the lowest datum still within 1.5 IQR of the lower quartile and the highest datum still within 1.5 IQR of the upper quartile.**(c)** Same as in (b) but selected transcription factors and regulatory proteins are shown. Box plot elements are defined as in Fig. 2b **(d)** Naïve $CD4^+$ T cells were treated with 50 μg/ml cycloheximide (CHX, blue points) and analyzed by flow cytometry at different time points. Shown is the fluorescence intensity relative to control cells that were not treated with CHX. n=3 from three different donors. Bars indicate the S.D. of the mean. **(e)** Naïve $CD4^+$ T cells were electroporated with Cas9, ATTO550-labeled tracrRNA and two sgRNA targeting the *B2M* locus. Cells were stained with an antibody to HLA-A/B/C and analyzed by flow cytometry 24 h and 72h after electroporation. NT: Non-targeting sgRNA control. The experiment was repeated three times with similar results.

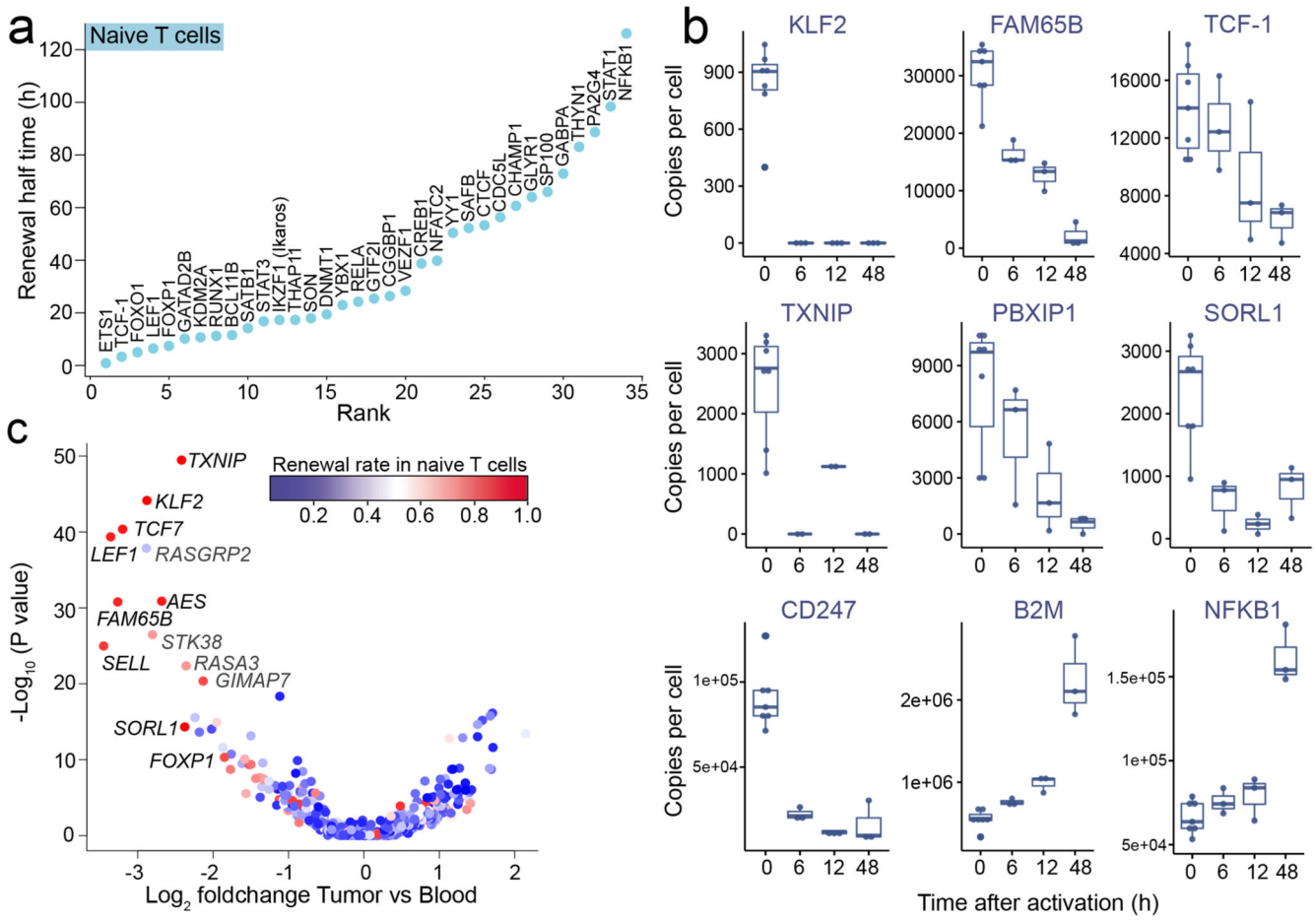

Fig. 3. Rapid turnover and tunability of transcription factors

(a) Ranking of transcription factors in naïve T cells according to the renewal half time. Average values from n=3 are shown **(b)** Time course ofthe abundances of selected proteins in copy numbers per cell. Data points that were identified by MS/MS are shown. Each dot represents a different donor. n=7 for naïve, resting T cells. n=3 for 6h, 12h, 48h activated T cells. Box plot elements are defined as in Fig. 2b **(c).** Volcano plot showing results from differential expression analysis (two-tailed Welch's t test) between mRNA levels in circulating (n=1627) and tumor-infiltrating $CD4^+$ T cells (n=2170). Data were from Zheng et al. 2016. Shown are only mRNAs for which the turnover rate of the corresponding proteins was determined. mRNAs that are induced in TILs, i.e. PD-1 are not shown as these proteins are not present in naïve T cells and accordingly no turnover rate could be determined. The color code shows the protein turnover rate according to the pulsed SILAC data shown in Fig. 1c. n=3 from three different donors.

Europe PMC Funders Author Manuscripts

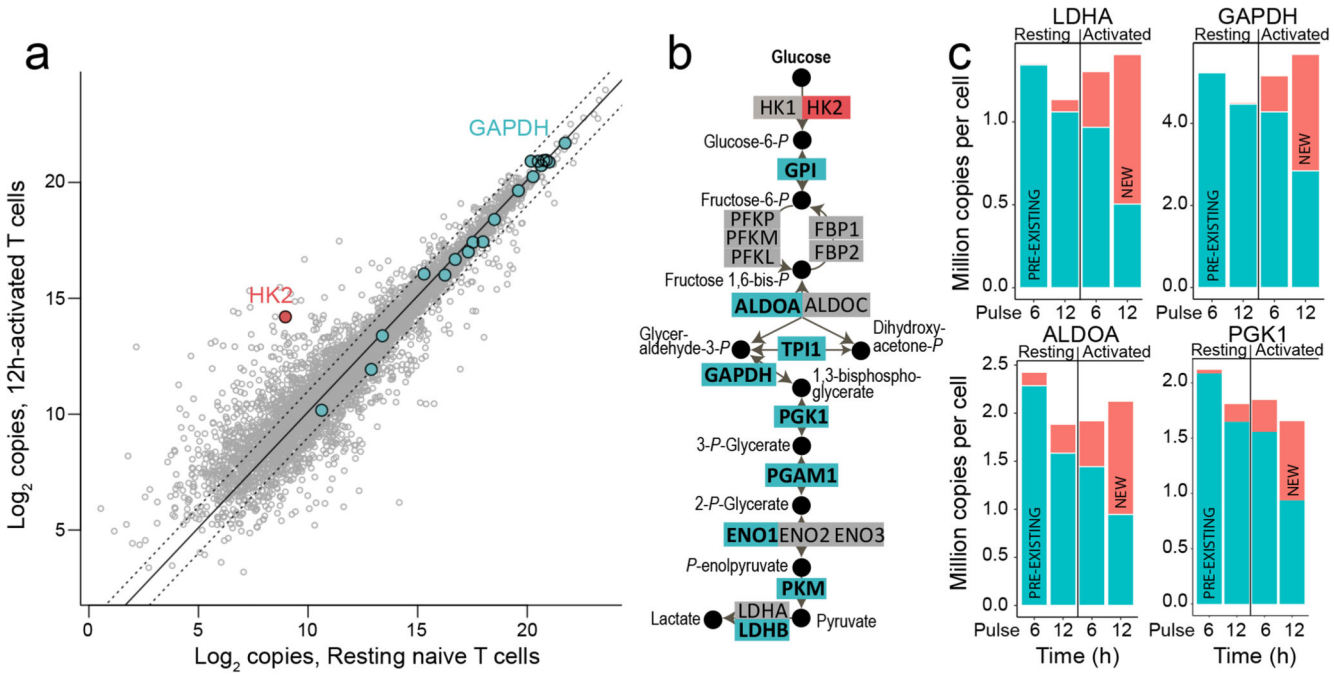

Fig. 4. Metabolic preparedness of T cells.

(a) Comparison of protein copy numbers in naïve and 12 h-activated CD4$^+$ T cells. Each dot represents a protein. Average values from n=7 for naïve and n=3 for 12h-activated T cells are shown. Glycolytic enzymes are shown as turquois dots. Hexokinase-2 (HK2) is marked in red. **(b)** Illustration of the glycolytic pathway. Highly abundant (> 300,000 copies) proteins in naïve T cells are shown in turquois. **(c)** The barplots show the fraction of pre-existing (turquois) and newly synthesized proteins (red) after a 6h and 12h pulse in naïve and activated T cells. Average values from n=3 are shown. Examples of LDHA, GAPDH, ALDOA and PGK1 are shown.

Europe PMC Funders Author Manuscripts

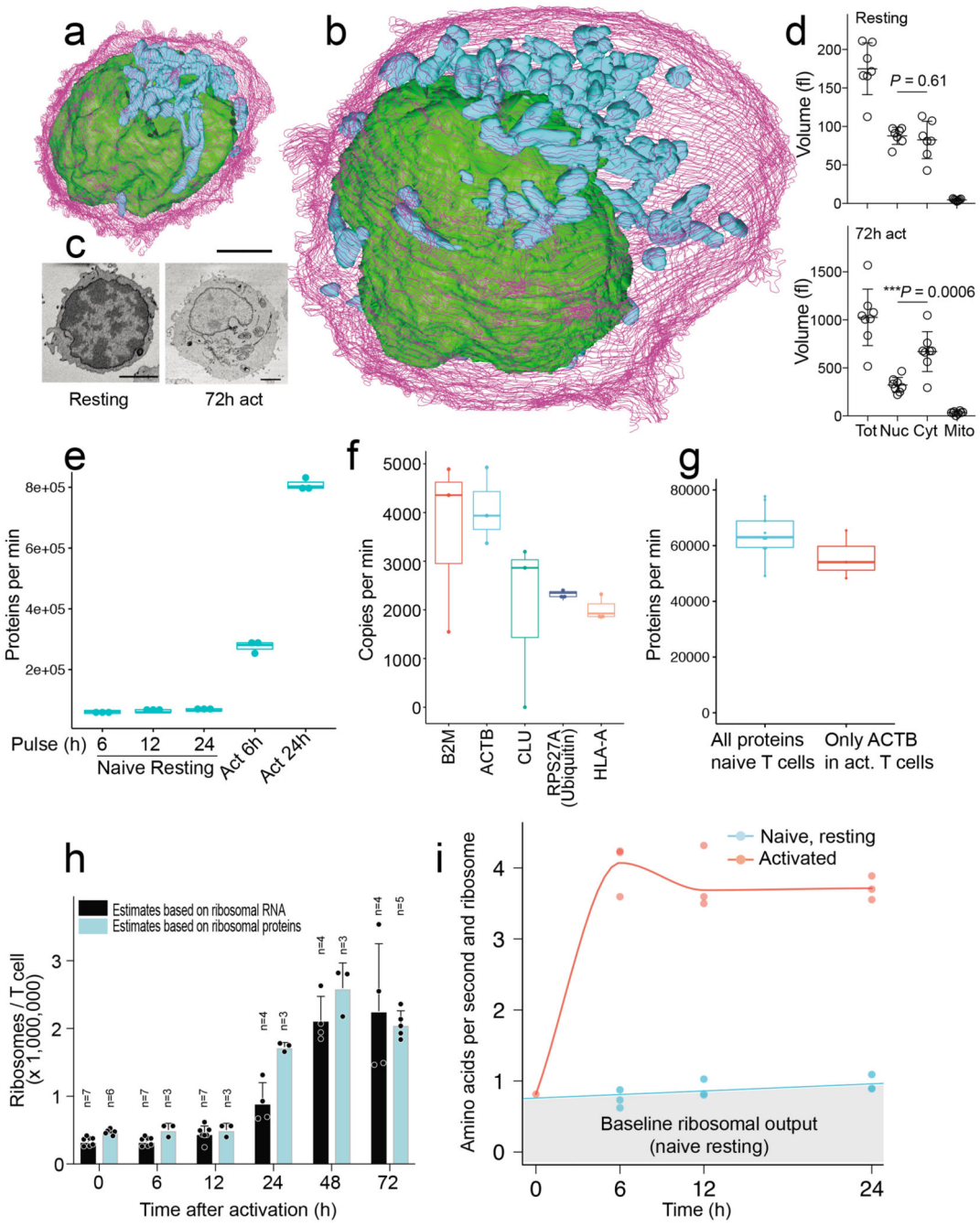

Fig. 5. Translational preparedness of naïve T cells.

(a) 3D reconstruction of a naïve CD4$^+$ T cell based on scanning block face electron microscopy images. The plasma membrane is drawn in purple, the nucleus in green and mitochondria in blue. Scale bar = 2 μm **(b)** 3D reconstruction of a 72 h-activated CD4$^+$ T cells. Both cells (A+B) are drawn at the same scale. **(c)** Examples of electron microscopy images of a naïve (left) and 72 h-activated T cell (right) that were used for the 3D reconstructions. A total of 7 naïve and 8 activated T cells were analyzed and quantified in (d). All cells were fixed and embedded together. Scale bar = 2 μm **(d)** Quantification ofcell

and organellar volumes based on 3D reconstructions of naïve $CD4^+$ and 72h-activated T cells. n=7 for naïve T cells, n=8 for 72h-activated T cell. Bars indicate the S.E.M. P values were determined by a two-tailed unpaired t-test. **(e)** Thenumber oftotal proteins that aresynthesized in a minute in resting, naïve and activated $CD4^+$ T cells are shown. For resting cells, data from three different pulse durations (6h, 12h, 24h) are shown. n=3 from three different donors. Box plot elements are defined as in Fig. 2b **(f)** Boxplot showing the synthesis rates of the five proteins with highest synthetic rates in naïve T cells. n=3 from three different donors. Box plot elements are defined as in Fig. 2b **(g)** Comparison of the total protein synthesis in naïve T cells tosynthesis of Actin B in 24h-activated T cells. n=7 for naïve, n=3 for memory. Box plot elements are defined as in Fig. 2b **(h)** Estimations of ribosomal proteins based on quantifications of ribosomal RNA and the median of ribosomal proteins.Sample numbers are indicated on the graph. Bars represent the S.E.M **(i)** Averagetranslation rate per ribosome in resting, naïve and activated $CD4^+$ T cells. n=3 from three different donors.

Europe PMC Funders Author Manuscripts

Europe PMC Funders Author Manuscripts

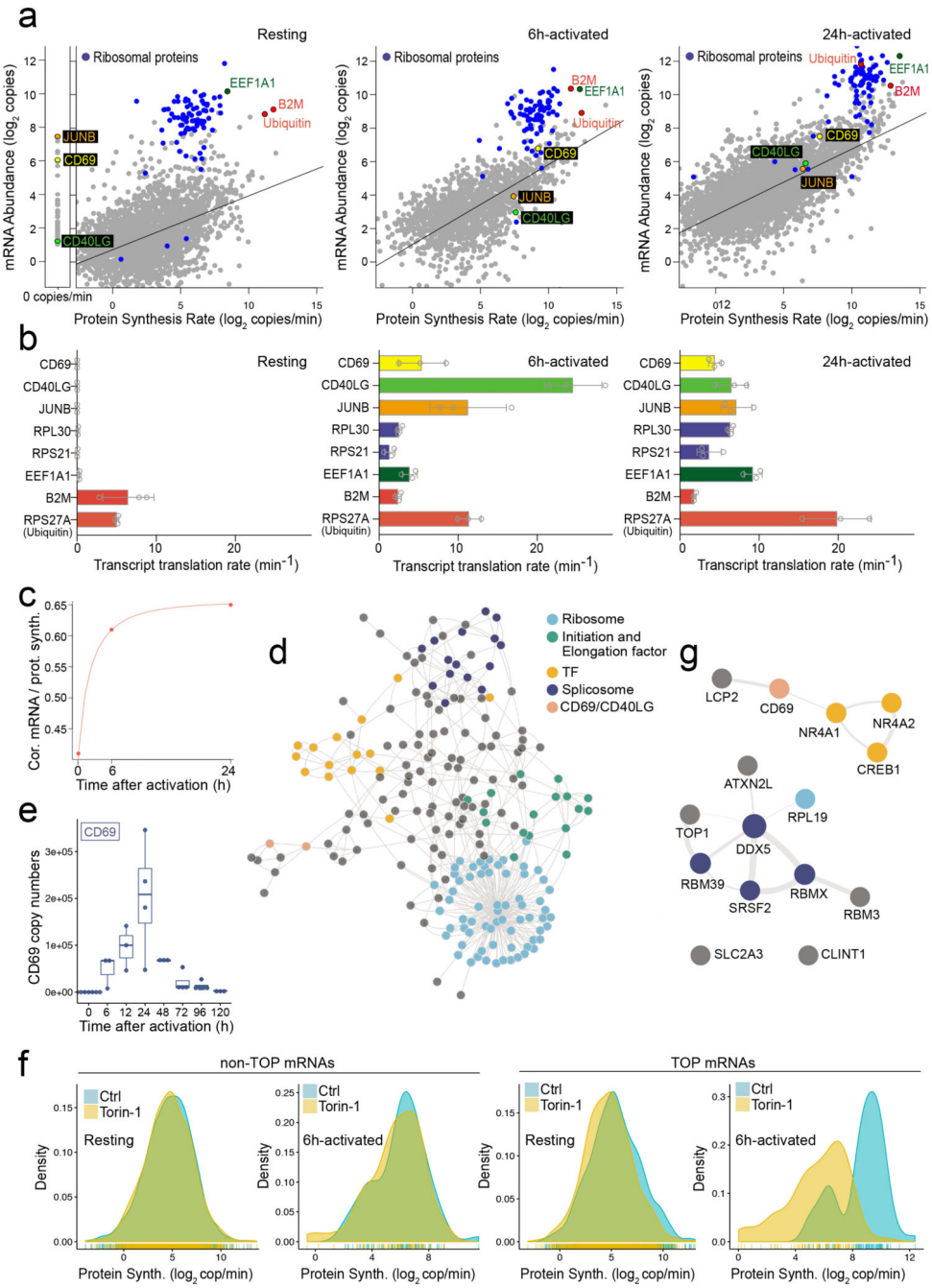

Fig. 6. Posttranscriptional regulations.

(a) Comparison ofabsolute mRNA copy numbers and average protein synthesis rates (from three donors) in resting (left panel), 6h-activated (middle panel) and 24h-activated T cells (right panel). Ribosomal proteins are colored in blue, all other colored dots are labeled with the protein name **(b)** Transcript translation rates of selected factors in resting (left panel), 6h-activated (middle panel) and 24h-activated T cells (right panel). Rates were calculated by dividing absolute protein synthesis rates by the number of respective mRNA copies. Theserates indicatehow many times a single transcript is read off by ribosomes per minute.

n=3 from three donors. Bars represent the S.E.M **(c)** Analysis of the Spearman's rank correlation between mRNA levels and protein synthesis rates in resting, 6 h and 24 h activated T cells. **(d)** Interaction network of proteins encoded by the 242 mRNAs that are repressed in naïve T cells. Each node represents a protein and edges represent protein-protein interactions based on the STRING database. **(e)** Absolute copy numbers of CD69 proteins in resting and activated T cells as determined by mass spectrometry. n=7 for naïve T cells,n=3 for 6h, 12h, 48h, 120h activated T cells,n=4 for 24h, 72h, 96h activated T cells. Box plot elements are defined as in Fig. 2b **(f)** Density plots showing the distribution of the protein synthesisrates (average from three different donors) in control T cells(blue) and T cells treated with 250 nM Torin 1 (yellow). The two panels on the left show the distribution of synthesis rates of proteins encoded by non-TOP mRNAs in naïve and 6h-activated T cells, respectively. The two panels on the right show the distribution of synthesis rates of proteins encoded by TOP mRNAs in naïve and 6h-activated T cells, respectively. **(g)** Subnetwork form Fig. 6d. The 15 nodes represent proteins encoded by repressed mRNAs that were engaged following activation independent on mTOR. The 15 mRNAs were identified by comparing activation-induced changes in synthesis rates of proteins that are encoded by the 242 repressed mRNAs. In the presence of Torin 1, the increase in the synthesis of these 15 proteins was not affected (Log2 Foldchange < 1). The color code is the same as in Fig. 6d.

Europe PMC Funders Author Manuscripts

Europe PMC Funders Author Manuscripts

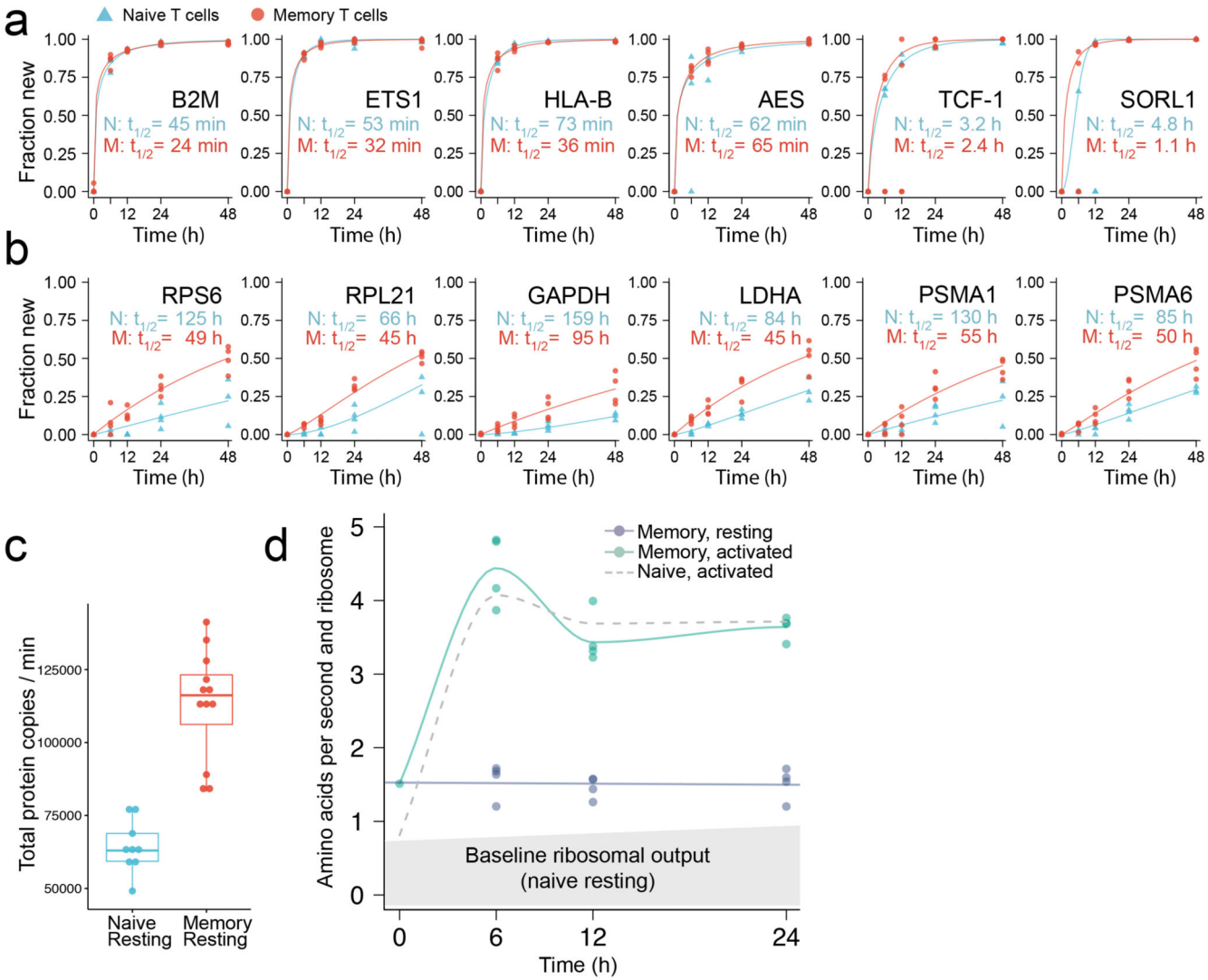

Fig. 7. Preparedness of memory T cells.

(a) Comparison of protein turnover kinetics in naïve and memory CD4$^+$ T cells of selected proteins. n=3 for naïve 6h and naïve 12h; n=4 for naïve 24h, memory 6h, memory 12h and memory 24hfrom different donors. **(b)** Same as in (a)but two ribosomal proteins (RPS6 and RPL21), two glycolytic enzymes (GAPDH and LDHA)and two proteasomal proteins (PSMA1 and PSMA6) are shown. **(c)** Comparison oftotal protein synthesis in resting, naïve and memory T cells.n=9 for naïve, n=12 for memory. Box plot elements are defined as in Fig. 2b **(d)** Averagetranslation rate per ribosome in amino acids per second and ribosome in resting, memory and activated CD4$^+$ T cells. The grey area shows the baseline ribosomal output in naïve T cells. n=4from threedifferent donors.